



HAL
open science

Temporal trends of legacy and novel brominated flame retardants in sediments along the Rhône River corridor in France

Sophia Vauclin, Brice Mourier, André-Marie Dendievel, Philippe Marchand, Anaïs Vénisseau, Amandine Morereau, Hugo Lepage, Frederique Eyrolle, Thierry Winiarski

► To cite this version:

Sophia Vauclin, Brice Mourier, André-Marie Dendievel, Philippe Marchand, Anaïs Vénisseau, et al.. Temporal trends of legacy and novel brominated flame retardants in sediments along the Rhône River corridor in France. *Chemosphere*, 2021, 271, pp.129889. 10.1016/j.chemosphere.2021.129889 . hal-03147392

HAL Id: hal-03147392

<https://hal.science/hal-03147392v1>

Submitted on 9 Apr 2021

HAL is a multi-disciplinary open access archive for the deposit and dissemination of scientific research documents, whether they are published or not. The documents may come from teaching and research institutions in France or abroad, or from public or private research centers.

L'archive ouverte pluridisciplinaire **HAL**, est destinée au dépôt et à la diffusion de documents scientifiques de niveau recherche, publiés ou non, émanant des établissements d'enseignement et de recherche français ou étrangers, des laboratoires publics ou privés.



Distributed under a Creative Commons Attribution - NonCommercial - NoDerivatives 4.0 International License

Temporal trends of legacy and novel brominated flame retardants in sediments along the Rhône River corridor in France

Sophia Vauclin^{1*}, Brice Mourier¹, André-Marie Dendievel¹, Philippe Marchand², Anaïs
Vénisseau², Amandine Morereau³, Hugo Lepage³, Frédérique Eyrolle³ & Thierry Winiarski¹

¹Univ Lyon, Université Claude Bernard Lyon 1, CNRS, ENTPE, UMR 5023, LEHNA, F-69518, Vaulx-en-Velin, France

²ONIRIS, INRAE, LABERCA Route de Gachet-Site de la Chantrerie-CS 50707, Nantes, F-44307, France

³Institut de Radioprotection et de Sûreté Nucléaire (IRSN), PSE-ENV/SRTE/LRTA, BP 3, 13115, Saint-Paul-lez-Durance, France

*Corresponding author: sophia.vauclin@developpement-durable.gouv.fr

Highlights :

- Time trends of legacy BFRs in sediments along the Rhône River are similar.
- Legacy BFRs reached their peak between the 1970s and the 2000s, and are now stable.
- nBFRs concentrations are two to four times lower than that of legacy BFRs.
- Some nBFRs appeared along the Rhône River as early as the 1970s-1980s.
- No decreasing trend in nBFRs concentrations has been observed, so far.

1 **Keywords:** Brominated flame retardants; contamination trend; polychlorinated biphenyls; Rhône
2 River; sediment core.

4 **Abstract**

5 Brominated flame retardants (BFRs) are anthropogenic compounds that are ubiquitous in most
6 manufactured goods. Few legacy BFRs have been recognised as persistent organic pollutants (POPs)
7 and have been prohibited since the 2000s. However, most BFRs continue to be used despite growing
8 concerns regarding their toxicity; they are often referred to as novel BFRs (nBFRs). While
9 environmental contamination due to chlorinated POPs has been extensively investigated, the levels
10 and spatiotemporal trends of BFRs are comparatively understudied. This study aims to reconstruct the
11 temporal trends of both legacy and novel BFRs at the scale of a river corridor. To this end, sediment
12 cores were sampled from backwater areas in four reaches along the Rhône River. Age-depth models
13 were established for each of them. Polychlorinated biphenyls (PCBs), legacy BFRs (polybrominated
14 diphenyl ethers - PBDEs, polybrominated biphenyls - PBBs and hexabromocyclododecane - HBCDDs)
15 and seven nBFRs were quantified. Starting from the 1970s, a decreasing contamination trend was
16 observed for PCBs. Temporal trends for legacy BFRs revealed that they reached peak concentrations
17 from the mid-1970s to the mid-2000s, and stable concentrations by the mid-2010s. Additionally,
18 individual concentrations of nBFRs were two to four orders of magnitude lower than those of legacy
19 BFRs. Their temporal trends revealed that they appeared in the environment in the 1970s and 1980s.
20 The concentrations of most of these nBFRs have not decreased in recent years. Thus, there is a need
21 to comprehend the sources, contamination load, repartition in the environment, and toxicity of nBFRs
22 before their concentrations reach hazardous levels.

23 **1. Introduction**

24 Brominated flame retardants (BFRs) are a group of anthropogenic molecules that are manufactured to
25 prevent or slow down the development of fire (WHO, 1997). Their production began in the 1960s and
26 1970s (Prevedouros et al., 2004; Jinhui et al., 2017). Since then, they have been incorporated in a wide

27 range of industrial processes and applications, including electronics, transportation, furniture (foams
28 and carpets), textiles, and construction (Alaee et al., 2003). Certain BFRs, namely polybrominated
29 diphenyl ethers (PBDEs), polybrominated biphenyls (PBBs), hexabromocyclododecanes (HBCDDs) and
30 tetrabromobisphenol A (TBBPA) are regarded as “established” or “legacy” BFRs. This is because they
31 have been identified in environmental matrices worldwide (De Wit, 2002; Law et al., 2003; Law et al.,
32 2006; De Wit et al., 2010; Guerra et al., 2012; Li et al., 2015), and their persistence and toxicity have
33 been assessed and acknowledged. They generally exhibit low acute toxicity but significant chronic
34 toxicity, leading to liver, kidney, and thyroid disorders (PBDEs and HBCDDs), development and
35 neurobehavioral issues in children (PBDEs and HBCDDs), reproductive disorders, digestive system
36 cancer, and lymphoma (mainly PBBs) (Darnerud et al., 2003; Kim et al., 2014). As a result, most legacy
37 BFRs have been progressively classified as persistent organic pollutants (POPs) in the Stockholm
38 Convention. Tetra and penta-BDE (commercial penta-BDE mixture) was classified in 2009, whereas
39 deca-BDE commercial mixture was classified in 2017 (Annex A of the Stockholm Convention, 2018).
40 This delay in addition is because legacy BFRs are not as well-studied as other pollutants, such as
41 chlorinated compounds (e.g. polychlorinated biphenyls [PCBs], dioxins, furans, and organochlorine
42 pesticides), which are regulated in Europe through the Water Framework Directive (2000/60/EC). The
43 global production of BFRs has reached the same order of magnitude as some of the chlorinated
44 compounds, such as PCBs. The production of PCBs reached its peak in the late 1960s at approximately
45 80 kt year⁻¹ (Breivik et al., 2002a), the global production of PBDEs global production peaked in 2002,
46 also around 80 kt (Abbasi et al., 2019). Nevertheless, health and environmental concerns linked to
47 legacy BFRs have led to a steady decline in their production and use over time. PBBs were produced
48 up until 1976 in the USA, 1977 in Germany, 1985 and the United Kingdom, and 2000 in France (IARC,
49 2016). Most commercial mixes of PBDEs have been prohibited by the European Union (EU) in the
50 electronic and electric industries from 2002 (2002/95/CE). Furthermore, the global production of
51 HBCDDs reportedly peaked in 2006 at 22 kt, most of the produced HBCDDs being used in the EU;
52 however, their production has seen a decline ever since (Koch et al., 2015).

53 As a result, numerous brominated compounds have replaced legacy BFRs and have gained attention
54 from the scientific community. According to Bergman et al. (2012), these replacement BFRs should be
55 referred to as “emerging BFRs” if they are present in the environment and/or in wildlife, humans or
56 other biological matrices, and as “novel BFRs” (nBFRs) if they are documented as potential flame
57 retardants in materials or products. Although the term “emerging BFRs” is rarely used in the literature,
58 the term “nBFRs” is commonly used (Poma et al., 2014; McGrath et al., 2017; 2018; Ganci et al., 2019;
59 Xiong et al., 2019). Therefore, this paper uses the term “novel BFRs” to designate BFRs which are new
60 to the market or have recently been observed in the environment, as defined by Covaci et al. (2011).
61 The European Food Safety Authority (EFSA, 2013) has identified twenty-seven nBFR compounds,
62 including pentabromoethylbenzene (PBEB), pentabromotoluene (PBT), and tetrabromo-o-
63 chlorotoluene (TBCT). Similar to legacy BFRs, nBFRs are used in many products such as textiles, plastics,
64 foams, and electrical cable coatings (Xiong et al., 2019). Furthermore, they have been identified in
65 many environmental matrices including air (Möller et al., 2011; Yu et al., 2015), wastewater (Cristale
66 et al., 2015; Li et al., 2018), indoor dust (Hassan et Shoeib, 2015; McGrath et al., 2018), sediments and
67 soils (Shi et al., 2009; La Guardia et al., 2013), and biota (Vetter et al., 2017; Vénisseau et al., 2018).
68 Additionally, nBFRs have been shown to bioaccumulate in some species (Wu et al., 2011; Zhang et al.,
69 2011). Existing toxicological studies suggest that they may cause various adverse effects (endocrine
70 disruption, neurotoxicity, DNA damage) at high exposure; however, information on their effects due
71 to chronic exposure at low concentrations is still scarce (Xiong et al., 2019).

72 It is essential to investigate the temporal trends of anthropogenic chemicals in environmental matrices
73 in order to evaluate their potential risks and to assess the need to regulate their production and use.
74 If a regulation is already in place, it is imperative to comprehend its lag time and effectiveness in
75 reducing the concentrations of contaminants in the environment. For this purpose, sediment deposits
76 are valuable natural archives of the anthropogenic contamination of hydrosystems. They are especially
77 relevant when investigating lipophilic contaminants (i.e., POPs), such as BFRs that tend to accumulate
78 in sediments (de Wit, 2002). Numerous sediment records have been successfully used to reconstruct

79 the temporal trends of PCBs. Moreover, various studies have shown that their worldwide prohibition
80 in the 1980s led to a significant decrease in their environmental concentrations (Chi et al., 2007;
81 Desmet et al., 2012; Bigus et al., 2014 Cui et al., 2016; Dendievel et al., 2020). However, their stocks
82 might continue to persist in sediments and could pose a risk of intermittent contaminant releases in
83 hydrosystems. As compared to PCBs, studies on the temporal trends of BFRs in sediments uncommon.
84 Most studies on BFRs focus on PBDEs (Baltic Proper: Nylund et al., 1992; Tokyo Bay: Minh et al., 2007;
85 Scotland: Muir and Rose, 2007; Switzerland: Kohler et al., 2008; Japan and Southern China coasts:
86 Tanabe, 2008; Sydney Estuary: Drage et al., 2015; Seine River: Lorgeoux et al., 2016), as they are often
87 the predominant BFRs in terms of concentrations detected in the environment (Law et al., 2006; 2014).
88 Sediment records of HBCDDs (Kohler et al., 2008; Tanabe et al., 2008; Poma et al., 2014; Law et al.,
89 2014) and temporal trends of PBBs (Zhu and Hites, 2005) are even more scarce in the literature. So far,
90 most temporal records of BFRs are thus derives from cores from a single location; however, no
91 temporal study has been attempted at the scale of a whole river corridor. To the best of our
92 knowledge, among nBFRs, temporal trends of just decabromodiphenyl ethane [DBDPE] and 1,2-
93 Bis(2,4,6-tribromophenoxy)ethane [BTBPE] have been published to date (Yang et al., 2012; Poma et
94 al., 2014). The scarcity of recorded temporal evolution of nBFRs in environmental matrices is especially
95 concerning because they continue to be manufactured. Given the growing evidence of their hazardous
96 effect (e.g., persistence, bioaccumulation, and toxicity), their increasing concentrations in the
97 environment is not ideal.

98 Therefore, this study aims to fill knowledge gap in the literature regarding both legacy and novel BFRs
99 by 1) characterising the temporal and spatial trends of PCBs and legacy BFRs (PBDEs, PBBs, HBCDDs)
100 and 2) comparing the trends of legacy and novel BFRs in sediments over time, along the highly
101 anthropized Rhône River corridor. To this end, sediment cores were retrieved from secondary channels
102 as well as a dam reservoir in four distinct areas along the Rhône River. The cores were characterised
103 in terms of grain size and total organic carbon, and dated. Moreover, concentrations of PCBs, legacy

104 BFRs (PBDEs, PBBs, and HBCDDs), and seven nBFRs were quantified, allowing for the robust
105 reconstruction of temporal trends for both legacy and novel brominated flame retardants.

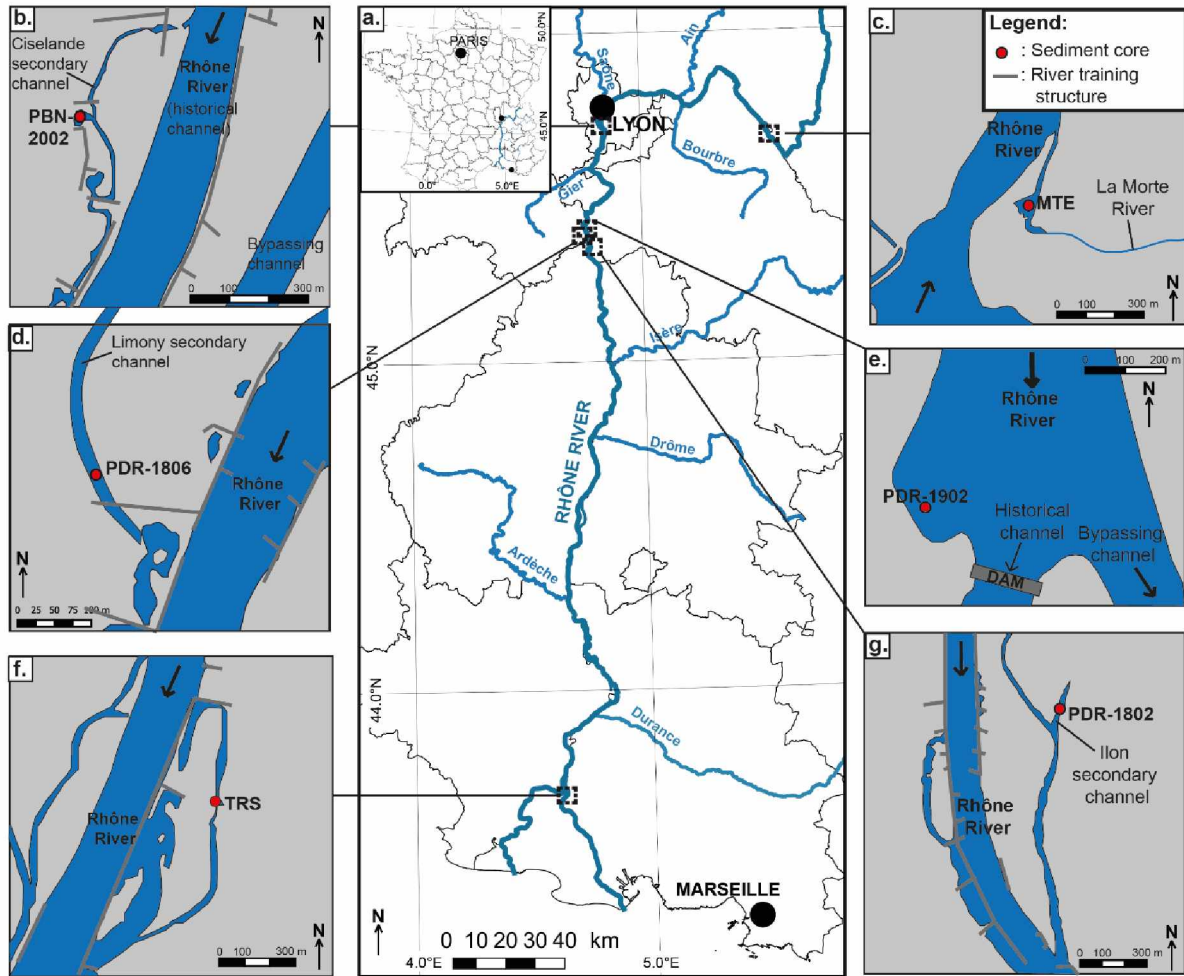
106 2. Geographic settings

107 2.1. Geographic context

108 The Rhône River is 812 km; it runs from the Valais region in Switzerland to the Mediterranean Sea in
109 France (Fig. 1.a). Its catchment covers an area of 98 500 km², of which 92 % is in France, and is mostly
110 mountainous (Olivier et al., 2009). With an average annual discharge of 1 690 m³ s⁻¹ close to its delta
111 (Arles), the Rhône is the largest river in France; moreover, in terms of discharge, it ranks eight in
112 Europe. It is also the most active river in France in terms of sediment transport, with a long-term mean
113 annual sediment load of approximately 6.6 x 10⁶ tons (Poulier et al., 2019) and a conveying speed of
114 approximately 2 km year⁻¹ (Pont et al., 2002).

115 The Rhône River catchment is highly anthropized. It supports a population of approximately 15.5
116 million that is mostly distributed along the river corridor. The river runs through major cities, including
117 Geneva (~1 million inhabitants) and Lyon (~1.4 million inhabitants), and through several industrial
118 areas. The largest industrial area in the region is the “Chemical Valley”, which is a 10 km-long reach
119 directly downstream of Lyon, comprising of numerous pharmaceutical, chemical, and petrochemical
120 industries. The river course has also been extensively engineered to facilitate navigation and to
121 produce hydroelectricity. There are numerous dykes and groynes constraining the river bed as well as
122 19 hydroelectric dams along the French section of the river, with one dam every 30 km on average
123 (Bethemont and Bravard, 2016).

124 2.2. Sampling sites



125

126 *Figure 1: a. Rhône River catchment with localisation of the study sites; b. PBN study site; c. MTE study site; d. PDR-1806 study*
 127 *site; e. PDR-1902 study site; f. TRS study site; g. PDR-1802 study site. [IN COLOUR]*

128 Six study sites located in four distinct areas were identified for this study (Fig. 1). Secondary channels,
 129 that is channels that are partly or entirely disconnected from the main channel most of the year, were
 130 selected as they represented steady waters environments (oxbow lakes, backwater areas). Sediment
 131 sequences in such environments are usually characterised by good preservation potential and
 132 continuity as well as high stratigraphic resolution (Bábek et al., 2008; Van Metre et al., 2008; Mourier
 133 et al., 2014), indicating that they might offer a reliable and high-resolution sediment record. The sites
 134 are described from upstream to downstream, as follows:

135 - MTE (Fig. 1.c), located approximately 415 km from the estuary, consists of a secondary channel
136 along the right bank, which is connected to the Rhône River at its downstream end and to a
137 small river (“La Morte”) at its upstream end (Fig. 1.c).

138 - PBN (Fig. 1.b): the area of Pierre-Bénite (PBN) is located 319 km away from the estuary and a
139 few kilometres downstream of the confluence of the Rhône and Saône rivers in Lyon. It is a
140 highly anthropized bypassed reach that runs along the “Chemical Valley”. The historical
141 channel is constrained by numerous groynes and dykes.

142 The site is selected for the study is an oxbow lake that was formed over time between two
143 groynes as they were progressively filled with sediments (Fig. 1.b). Under high discharge
144 conditions, it is connected to a secondary channel that was partly restored in 2000. The oxbow
145 lake has never been dredged.

146 - PDR (Fig. 1.d, e, g): the area of Péage-de-Roussillon (PDR) is located 278 km from the estuary
147 and approximately 50 km downstream of Lyon. It is a 12 km-long reach organised in a bypassed
148 configuration that is typical of the Rhône River: an artificial canal equipped with a hydroelectric
149 power plant has been dug out to improve navigation and produce electricity, while the
150 historical channel has been dammed to obtain most of the discharge in the canal. The old
151 channel is also equipped with river training infrastructures (dykes and groynes) that were built
152 in the 1880s to facilitate navigation on the Rhône River.

153 Additionally, three sites from the historical channel were studied to include diverse
154 depositional environments, and therefore varying time periods and contamination patterns
155 recorded in the sediments:

- 156 ○ The dam reservoir (core PDR-1902, located 278 km from the estuary; Fig. 1.e) was built
157 between 1974 and 1978. It is a run-of-river dam, implying that it can be removed
158 during floods to allow high discharges. However, a small recess zone on the right bank
159 has allowed continuous accumulation of sediment since the construction of the dam,
160 as proved by bathymetric surveys of the reservoir over time (Vauclin et al., 2020).

- 161 ○ The Limony secondary channel is located on the right bank (core PDR-1806, located
162 273 km from the estuary; Fig. 1.d). It was disconnected due to the implementation of
163 artificial embankments in the 1880s. Currently, it is mostly supplied by groundwater
164 and is occasionally connected to the main channel during floods.
- 165 ○ The Ilon secondary channel (core PDR-1802, located 272 km from the estuary; Fig. 2.g)
166 is located on the left bank of a larger secondary channel. Its upstream end was
167 disconnected following the drastic discharge reduction caused by the implementation
168 of the dam in 1978. However, the channel is still underwater throughout the year,
169 supplied by its downstream end.

170 To decipher the variations in temporal concentrations, the results from this area are site-
171 specific. However, to understand spatial trends, they are studied from an overarching
172 perspective, as sites are located only a few kilometres apart.

- 173 - TRS (Fig. 1.f): this site is located approximately 275 km downstream from Lyon and 54 km
174 upstream from the estuary into the Mediterranean Sea, therefore it represents the river
175 catchment as a whole. It consists of a secondary channel, wherein the entrances were barred
176 by a combination of dykes and groynes in the late 19th century (Fig. 1.f). Consequently,
177 sediments accumulation led to migrating sandbars in the secondary channel.

178

179 3. Material and methods

180 3.1. Sediment cores sampling and general characterisation

181 One core was sampled from each study site (Fig. 1). Characteristics of all the cores, except PBN-2002,
182 have already been published in other papers, although the data on BFR contamination from these
183 cores are mostly original. Furthermore, data on MTE and TRS were published by Morereau et al. (2020),
184 and those for PDR-1802, PDR-1806, and PDR-1902 were published by Vauclin et al. (2020).

185 The core locations were systematically chosen after conducting on-site ground penetrating radar (GPR)
186 surveys and analysing them. The cores were positioned to include a significant layer of sediments as
187 well as interesting subsurface structures identified on the GPR profiles. All cores, except PDR-1806 (Fig.
188 1.d) and TRS (Fig. 1.f) were sampled underwater from a flat-bottomed polyethylene boat using a
189 UWITEC® gravity corer (Uwitec, Mondsee, Austria) fitted with a 2 m long and 63 mm diameter plastic
190 liner. Cores PDR-1806 and TRS were sampled when their respective secondary channels were in a
191 dewatered state. A Cobra TT percussion driller equipped with a 40 mm-diameter transparent PVC liner
192 was used in the case of PDR-1806, and a 90 mm-diameter liner was used in the case of TRS.

193 The position and characteristics of the six cores are summarised in the Supplementary Material (SI-1).
194 Grain size was measured in all cores every 0.5 cm (PDR-1902), 1 cm (PDR-1806, PDR-1802, PBN-2002),
195 or 4–8 cm (TRS and MTE) in the LEHNA laboratory (Lyon, France) with a Mastersizer 2000© (Malvern
196 Panalytical) particle size analyser mounted with a hydro SM small volume dispersion unit. Descriptive
197 grain-size statistics (D50, mode, D10, D90, skewness, etc.) were computed using the Gradistat v.8
198 software (Blott and Pye, 2001). To represent the grain-size distributions, heatmaps of each core were
199 plotted; for each measured sample, the percentage of each grain-size class was represented using a
200 colour scale (SI-4).

201 Rock-Eval pyrolysis was used to analyse the total organic carbon (TOC) in all the studied cores with a 4
202 cm step (SI-4). The analyses were carried out in the ISTO laboratory (Orléans, France) using a Turbo 6
203 Rock-Eval pyrolyser (Vinci Technologies).

204 3.2. Contaminants analysis

205 The following organic contaminants were quantified in the LABERCA laboratory (ONIRIS Nantes,
206 France):

207 - Seven indicator polychlorinated biphenyl (PCB) congeners: PCB 28, 52, 101, 118, 138, 153, and 180;
208 their sum is $\sum 7\text{PCBi}$.

209 - Eight polybrominated diphenyl ether (PBDE) congeners: PBDE 28, 47, 99, 100, 153, 154, 183, and 209,
210 with their sum being Σ 8PBDE.

211 - Three polybrominated biphenyl (PBB) congeners: PBB 52, 101, and 15; their sum is Σ 3PBB.

212 - Three hexabromocyclododecane (HBCDD) stereoisomers: α , β , and γ ; their sum is Σ 3HBCDD.

213 - Seven novel BFRs (nBFRs): 1,2,3,5,4-pentabromobenzene (PBBz), pentabromotoluene (PBT), 2, 3, 5,
214 6-tetrabromo-p-xylene (TBX), hexabromobenzene (HBB), pentabromoethylbenzene (PBEB),
215 tetrabromo-o-chlorotoluene (TBCT), and octabromotrimethylphenylindane (OBTMPI). Note that the
216 nBFRs presented in this paper are abbreviated according to the harmonised list of abbreviations
217 proposed by Bergman (2012), except for PBBz, which does not appear in the list.

218 PCBs, PBDEs, and PBBs were quantified in all the cores, HBCDDs were quantified in all the cores except
219 PDR-1902 and PBN-2002, and nBFRs were quantified only in PDR (three cores) and PBN (one core)
220 areas.

221 The samples were collected at a 4–8 cm steps, packaged in amber glass vials and sent to the LABERCA
222 laboratory for further analysis. For each sample, pressurised liquid extraction was performed on 2 g of
223 sediment, using a Büchi system (Büchi, Rungis, France) and a mixture of toluene/acetone as solvent
224 (70/30, v/v) (Liber et al., 2019). Three purification steps were performed using acidic silica, Florisil®,
225 and celite/carbon columns, successively (Liber et al., 2019). HBCDD stereoisomers were analysed using
226 liquid chromatography with tandem mass spectrometry (LC-MS/MS). All the other persistent organic
227 pollutants (POPs) analyses were simultaneously carried out by gas chromatography coupled with high-
228 resolution mass spectrometry (GC/HRMS) using a 7890A gas chromatograph (Agilent) coupled with a
229 JMS 800D double-sector high-resolution mass spectrometer (JEOL, Tokyo, Japan) with three injections:
230 (1) PCBs, (2) deca-BDE and OBTMPI, and (3) PBBs, the remaining 7 PBDEs, and the remaining 6 nBFRs.
231 Quantification was ensured by isotopic dilution of seven ^{13}C -labeled internal PCB standards, eight ^{13}C -
232 labeled internal PBDE standards, and three ^{13}C -labeled internal HBCDD standards added to the
233 samples before the extraction step. For the nBFRs, ^{13}C -labeled internal standards were used for HBB

234 and PBBz, while PBT, TBX, PBEB, and TBCT were quantified with regard to the PBBz standard. Finally,
235 the OBTMPI was quantified with respect to the BDE-209 standard as both compounds were in the
236 same elution fraction during purification and were injected in the same chromatographic column. A
237 thorough description of the protocol can be found in Vénisseau et al. (2015) and Liber et al. (2019).
238 A procedural blank (consisting of a celite matrix) and an internal quality control (QC) standard were
239 included in each batch of the ten samples. The associated in-house charts were in accordance with the
240 acceptable limits fixed for these QC runs, that is, set at $\pm 2\sigma$ of the average value. The analytical
241 methods were conducted according to ISO 17025 standards; the QA/QC requirements were fulfilled
242 throughout the study. Furthermore, the laboratory has continuously participated in proficiency tests
243 on PCBs and PBDEs with acceptable results (Z-score $b \pm 2$). The limits of detection (LODs) ranged from
244 0.049 (PCB 118) to 0.109 (PCB 28) $\mu\text{g kg}^{-1}$ dry weight (DW) for PCBs, 0.00002 (PBDE 28) to 0.05 (PBDE
245 183) $\mu\text{g kg}^{-1}$ DW for PBDEs, 0.00005 (PBB 52) to 0.0062 $\mu\text{g kg}^{-1}$ DW (PBB 101) for PBBs, 0.002 to 0.136
246 $\mu\text{g kg}^{-1}$ DW for HBCDDs, and 0.00001 (TBCT and PBT) to 0.0482 (OBTMPI) $\mu\text{g kg}^{-1}$ DW for nBFRs.

247 3.3. Sediment core dating

248 The age-depth models of MTE and TRS cores have been published by Morereau et al. (2020) and
249 Dendievel et al. (2020). Furthermore, the age-depth models of cores PDR-1802, PDR-1806, and PDR-
250 1902 were published by Vauclin et al. (2020). The model for core PBN-2002 is original but based on the
251 multi-proxy methodology developed by Vauclin et al. (2020). Details regarding the modelling inputs
252 and parameters for PBN-2002 are provided in the Supplementary Material (SI-3).

253 4. Results and discussion

254 4.1. Sediment characteristics and dating

255 4.1.1. Grain-size characteristics

256 Grain-size characteristics as well as the TOC content of the six sediment cores are available in the
257 Supplementary Information (SI-3). Grain-size distributions in cores MTE, PBN-2002, and PDR-1902 are

258 comparable: the sediments are silty (D50 ranging between 20 and 50 μm), poorly sorted (i.e., the
259 distribution is widely spread around the D50), and vertically homogeneous. This type of grain size is
260 optimal for studying contamination as POPs tend to bind strongly to fine particles (Karickhoff et al.,
261 1979). Furthermore, uniformity indicates that the grain size is unlikely to be a confounding factor
262 regarding vertical contamination trends. The top 50 and 80 cm of cores PDR-1806 and PDR-1802
263 displayed similar grain size characteristics (silty, poorly sorted and homogeneous), respectively, but
264 the bottom parts of these cores were composed of very fine to medium sands (D50 ranging from 100
265 to 500 μm). These differences in grain size reflect the evolution of the channels in which the cores are
266 sampled, ranging from a river channel (bottom part, coarser sediments) to an abandoned channel (top
267 part, finer sediments), as established by Vauclin et al. (2020). Finally, the grain size in the TRS core
268 constantly fluctuated between silt and fine sand (D50 mostly ranging from 10 to 100 μm).

269 4.1.2. Total Organic Carbon content

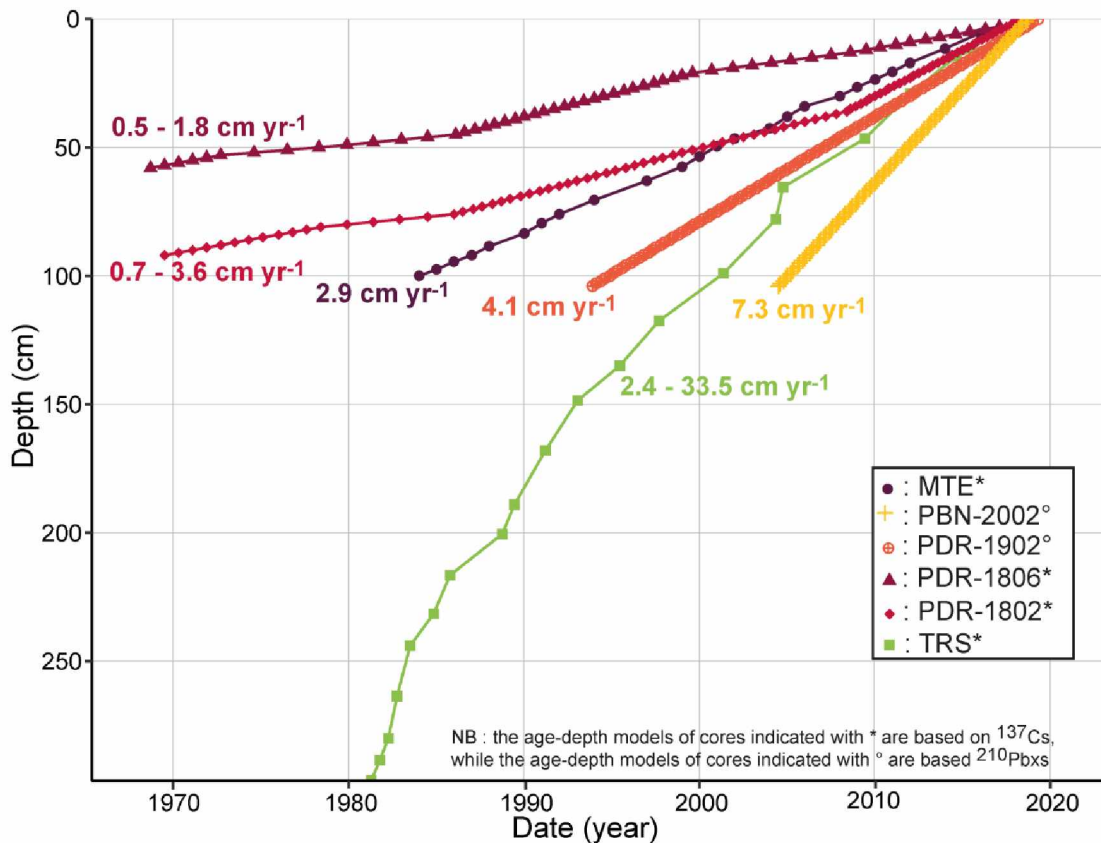
270 Total Organic Carbon content (TOC) ranged from 0 to 5% in the studied cores. It was vertically
271 homogeneous in MTE (2–3%), PBN-2002 (2–3%), PDR-1902 (~2%), and TRS (1–2%). It was slightly more
272 variable in the PDR-1802 core, such that it was around 1% at the bottom of the core where the
273 sediments were sandy; furthermore, it quickly increased to 3% at a depth of 60 cm, decreased, and
274 finally remained stable at approximately 2%. Finally, the most significant TOC variation was observed
275 in the PDR-1806 core, where the TOC was significantly low (< 1%) at the bottom of the core (up to 60
276 cm) in the presence of sandy sediments. Then, it increased steadily up to 4–5% close to the surface.
277 Organic carbon content is known to influence the affinity of organic contaminants for sediments;
278 additionally, because of their hydrophobic properties, POPs tend to bind to organic matter (Karickhoff
279 et al., 1979). As a result, TOC can be a confounding factor when examining vertical contamination
280 trends. Spearman correlation matrices were computed between the POP concentrations, the TOC and
281 the grain size (SI-8). They showed no significant relation between the TOC and the POP concentrations
282 for all cores except PDR-1806. The PDR-1806 core exhibited strong correlations between the TOC and

283 several contaminant concentrations (PBDEs, HBCDDs, HBB, PBBz, and TBX). Therefore, only the top 60
284 cm of the core was used for analysis, where variations in TOC were less.

285 4.1.3. Age-depth models

286 The age-depth models built for each core (Fig. 2) covered a time period ranging from 1970 to 2020.
287 PDR-1806 in its entirety had sediments from the 1930s, but the top 60 cm used for the contamination
288 trend comparison corresponds to a period ranging from 1968 to 2018. The different cores display
289 variable sedimentation rates related to the type of depositional environment they were sampled in.
290 PDR-1806 and PDR-1802 have the lowest accumulation rate, that is 0.5–1.8 cm yr⁻¹ and 0.7–3.6 cm yr⁻¹,
291 respectively, which is consistent with the fact that their filling mechanisms are characteristic of a
292 passive channel fill (Vauclin et al., 2020); moreover, they cover the longest time-period (1970–2018).
293 MTE displays a similar filling dynamic, that is a consistent sedimentation rate of around 2.9 cm yr⁻¹. It
294 covers a time-period ranging from 1985–2018. As PDR-1902 was sampled in an undisturbed dam
295 reservoir, it exhibited a stable and slightly higher sedimentation rate of approximately 4.1 cm yr⁻¹,
296 covering a time period from the early 1990s to 2019. PBN-2002 dated back to the early 2000s and
297 displayed a high accumulation rate of around 7.3 cm yr⁻¹. This sedimentation is probably linked to the
298 reactivation (dredging and reconnection in the early 2000s) of the secondary channel, which is
299 connected to the oxbow lake where the sediment core was sampled (refer to Section 2.1). Finally, TRS
300 had the highest and most fluctuating sedimentation rate out of the six cores, ranging from 2.4 to 33.5
301 cm yr⁻¹, with an average rate of 7.9 cm yr⁻¹. A sedimentation rate of 33.5 cm yr⁻¹ is extremely high. The
302 rates reported in the literature in similar hydromorphological contexts are usually lower: 0.65–2.4 cm
303 yr⁻¹ along the Ain River, France (Piégay et al., 2008), 0–2.6 cm yr⁻¹ in small rivers from the south-east
304 of France (Citterio and Piégay, 2009), 0.5–5.2 cm yr⁻¹ along the Wurm River, Germany (Hagemann et
305 al., 2019), and up to 7.7–8 cm yr⁻¹ along the Morava River, Czech Republic (Bábek et al., 2008; Sedláček
306 et al., 2016). However, the average sedimentation rate of core TRS (7.9 cm yr⁻¹) is consistent with some
307 of the reported values. In addition, most examples from the literature are from small or medium rivers,

308 while the TRS core is located close to the estuary of a major river known for its important sediment
 309 transport, and downstream of the confluence of the Rhône River with the Durance River, which has a
 310 high sediment load (Chapuis, 2012). In such a setting, dozens of centimetres of sediment can be
 311 deposited in a short amount of time during floods, which explains the occasionally high sedimentation
 312 rates.



313
 314 *Figure Error! No text of specified style in document.2: Age-depth models for the six studied sediment cores. Models for TRS*
 315 *and MTE were first published in Dendievel et al., 2020 and Morereau et al., 2020 while the models for PDR-1802, PDR-1806*
 316 *and PDR-1902 were first published in Vauclin et al., 2020. [IN COLOUR]*

317 4.2. Legacy BFRs in the Rhône River sediments

318 4.2.1. Contamination levels and congeners repartition

319 In this study, PCBs were selected as the “reference” POPs, as their levels and spatiotemporal trends in
 320 the Rhône River were extensively studied (Desmet et al., 2012; Mourier et al., 2014; Dendievel et al.,
 321 2020). They were quantified in 100% of the samples (Table 1). Their concentrations range from 0.22

322 $\mu\text{g kg}^{-1}$ DW in PDR to $194.72 \mu\text{g kg}^{-1}$ DW in TRS. Furthermore, based on the study area, their median
 323 concentrations ranged from $10.20 \mu\text{g kg}^{-1}$ DW in MTE, which is the most upstream site, to $41.13 \mu\text{g kg}^{-1}$
 324 DW in TRS, which is the most downstream site. A comprehensive PCB contamination study (Dendievel
 325 et al., 2020) showed that its median concentrations in the Upper Rhône (upstream of Lyon) was
 326 $15 \pm 10 \mu\text{g kg}^{-1}$ (consistent with MTE concentrations) and the Middle Rhône section (between Lyon and
 327 the Isère River confluence) was $32 \pm 24 \mu\text{g kg}^{-1}$ DW. This was consistent with the concentrations
 328 obtained in this study with respect to PBN and PDR. The seven congeners repartitions were similar in
 329 the six cores, with PCB-153 consisting of the highest proportion of $\sum 7\text{PCBi}$ (with an average of $\sim 28\%$
 330 for all six cores) and PCB-28 consisting of the lowest proportion ($\sim 4\%$ on average). The three highly
 331 chlorinated congeners (PCB-138, PCB-153, and PCB-180) represented approximately 70% of the total
 332 concentration, on average. This repartition is consistent with other observations from the Rhône River
 333 sediments (Desmet et al., 2012), given that lighter congeners are more prone to volatilization or
 334 microbial degradation than highly chlorinated compounds (Barriault and Sylvestre, 1993).

335 *Table 1: Occurrence, mean and median concentrations of PCBs and legacy BFRs according to the study area, in $\mu\text{g kg}^{-1}$ dry*
 336 *weight. The statistics were computed using all the values. DR = Detection rate; SD = standard deviation. LOD = limit of*
 337 *detection; NM = not measured.*

Contaminants	MTE (n = 25)			PBN (n = 27)			PDR (n = 72)			TRS (n = 20)		
	DR	Mean (SD)	Median (min-max)	DR	Mean (SD)	Median (min-max)	DR	Mean (SD)	Median (min-max)	DR	Mean (SD)	Median (min-max)
$\sum 7\text{PCBi}$	100%	12.07 (5.54)	10.20 (4.78– 23.96)	100%	21.83 (11.89)	19.0 (10.21– 62.27)	100%	32.55 (24.72)	30.79 (0.22– 114.60)	100%	73.21 (63.88)	41.13 (4.62– 194.72)
$\sum 8\text{PBDE}$	100%	7.00 (6.65)	4.94 (0.57– 30.11)	100%	136.18 (78.63)	131.99 (23.94– 287.87)	100%	84.78 (76.16)	108.11 (0.077– 376.73)	100%	28.99 (38.15)	13.33 (0.15– 125.15)

Σ3PBB	24%	0.0018 (0.003)	<LOD (<LOD – 0.0098)	89%	0.0043 (0.003)	0.0037 (<LOD– 0.013)	42%	0.0077 (0.014)	<LOD (<LOD– 0.075)	85%	0.016 (0.015)	0.0097 (<LOD– 0.048)
Σ3HBCD D	92%	0.60 (1.05)	0.29 (<LOD–5.3)	NM	NM	NM	71%	5.5 (8.96)	1.95 (<LOD– 41.95)	60%	0.84 (1.71)	0.13 (<LOD– 5.56)

338 PBDEs were also quantified in 100% of the samples, with concentrations ranging from 0.0077 $\mu\text{g kg}^{-1}$

339 DW (PDR) to 376.73 $\mu\text{g kg}^{-1}$ DW (PDR); their median concentrations per study area ranged from 5 μg

340 kg^{-1} DW in MTE to 132 $\mu\text{g kg}^{-1}$ DW in PBN. These concentrations were significantly higher than those

341 reported by Liber et al. (2019), wherein the median $\Sigma 8\text{PBDE}$ concentration was found to be 3.8 $\mu\text{g kg}^{-1}$

342 DW in the five cores obtained from the Rhône River, and by Lorgeoux et al. (2016), where the

343 maximum $\Sigma 8\text{PBDE}$ concentration in a core located downstream the Paris megacity was 60 $\mu\text{g kg}^{-1}$ DW.

344 However, similar or higher PBDE concentrations in sediments have been observed in Europe, mainly

345 in estuaries. The average PBDE concentration in the Scheldt estuary in the Netherlands and in the

346 Clyde estuary in the UK was 115 $\mu\text{g kg}^{-1}$ DW (Van Ael et al., 2012) and 287 $\mu\text{g kg}^{-1}$ DW (Vane et al.,

347 2010) respectively. The congener distribution was dominated by BDE-209, which represented 97% of

348 the total concentration on average. This is a very common observation in PBDE congener profiles all

349 over the world (Law et al., 2014). Moreover, it is consistent with the extensive worldwide use of the

350 commercial mixture “deca-BDE” (mostly composed of congener 209), which was prohibited after 2008

351 in the European Union, after the prohibition of other PBDE mixtures/congeners.

352 PBBs were quantified in 24%, 89%, 42%, and 85% of the samples in MTE, PBN, PDR, and TRS,

353 respectively. The concentrations were significantly lower than those of PCBs or PBDEs, ranging from

354 values below LOD to a maximum of 0.075 $\mu\text{g kg}^{-1}$ DW in PDR. However, they are in the same order of

355 magnitude as PBB-153 concentrations observed in Lake Michigan (0.11 $\mu\text{g kg}^{-1}$ DW) and the Lake Erie

356 (0.06 $\mu\text{g kg}^{-1}$ DW) (Zhu and Hites, 2005). PBB-153 represented in average 56% of the $\Sigma 3\text{PBB}$

357 concentrations in our samples, while PBB-101 and PBB-52 accounted for approximately 30% and 15%

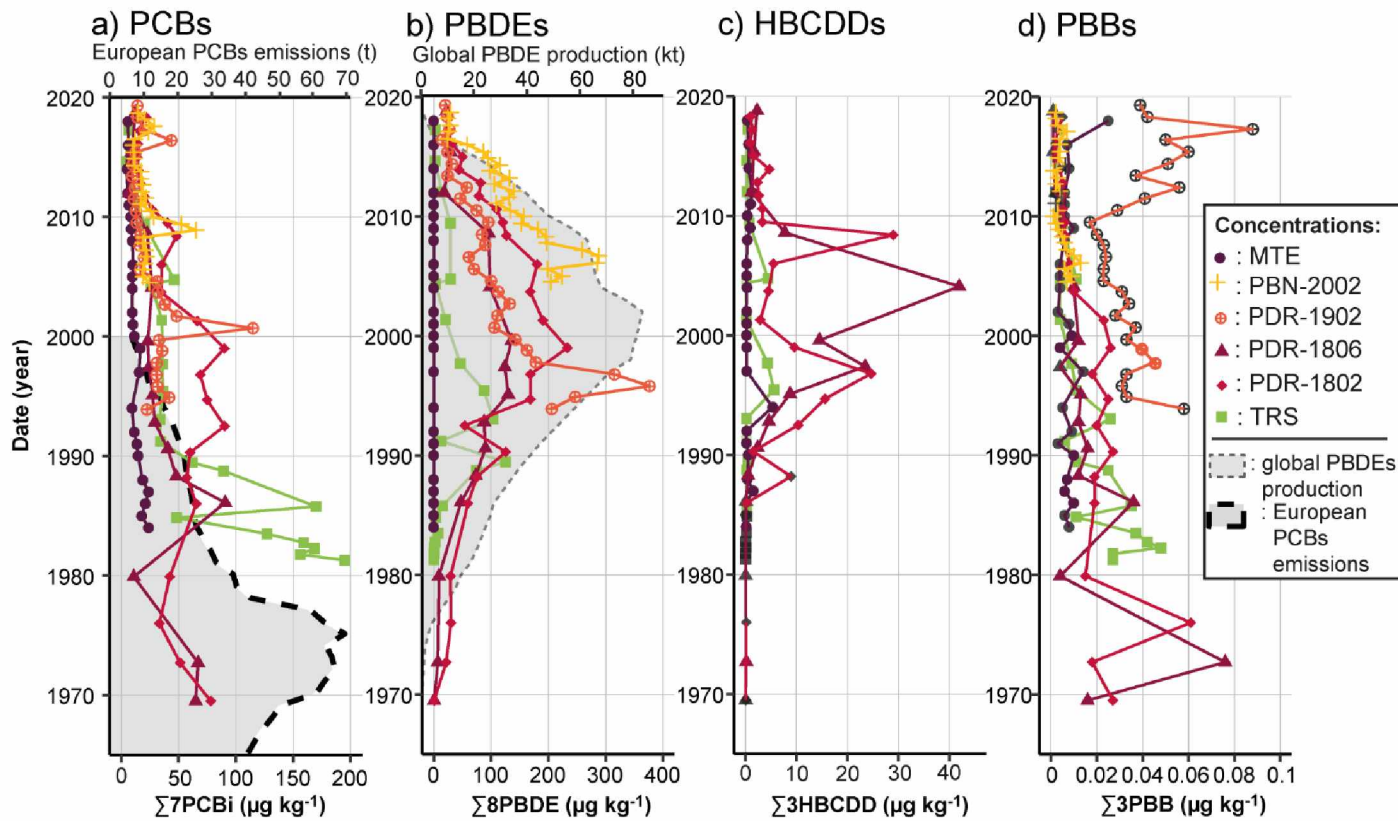
358 respectively. This is consistent with the fact that commercial PBB mixtures are mostly (60%–80%)
359 composed of hexabromobiphenyls, such as PBB-153 (Sundström et al., 1976).

360 HBCDDs were quantified in 92%, 71%, and 60% of the samples in MTE, PDR, and TRS, respectively.
361 Median concentrations per study area were relatively low, ranging from 0.13 $\mu\text{g kg}^{-1}$ DW in TRS to 1.95
362 $\mu\text{g kg}^{-1}$ DW in PDR, with the maximum concentration being observed in PDR, that is 41.95 $\mu\text{g kg}^{-1}$ DW.
363 Globally, these concentrations are of the same order of magnitude as those observed in the Garonne
364 Estuary (maximum concentration of 0.09 $\mu\text{g kg}^{-1}$ DW; Lauzent, 2017), Brisbane estuary (1 ± 1.5 $\mu\text{g kg}^{-1}$
365 DW; Anim et al., 2017), the Sydney estuary (1.8–5.3 $\mu\text{g kg}^{-1}$ DW; Drage et al., 2015), Lake Ellasjøen in
366 Norway (4 $\mu\text{g kg}^{-1}$ DW; Evenset et al., 2007) or even the Kuzuryu River in Japan, which receives effluents
367 from the textile industry (0.087–7.8 $\mu\text{g kg}^{-1}$ DW; Oh et al., 2014). However, higher HBCDD
368 concentrations were measured in the river and harbour of Tianjin in China (mean concentration: 31 μg
369 kg^{-1} DW; maximum: 634 $\mu\text{g kg}^{-1}$ DW; Zhang et al., 2013). On average, stereoisomer γ , α , and β
370 accounted for approximately 60%, 30%, and 10% of the total concentrations, respectively. This
371 distribution is consistent with results in the literature (Oh et al., 2014; Anim et al., 2017) and the
372 commercial HBCDD mixture formulation (Covaci et al., 2006; ANSES, 2017).

373 It should be noted that the legacy BFRs under consideration exhibited different levels of persistence in
374 sediments, which could partially explain the variation in their concentration ranges. BDE-209 had the
375 highest half-life of the three classes of BFRs, comprising approximately 2–4 years (Gerecke et al., 2005;
376 2006). PBBs reportedly had half-lives ranging from 3 to 290 days (FAO, 2000). Although HBCDDs are
377 classified as POPs, their half-lives in sediments ranged between 1 to 128 days (Davis et al., 2005; Marvin
378 et al., 2011). This is below the regulatory 6 months for an organic pollutant to be considered as
379 persistent. This may have enhanced the discrepancy between the concentration and detection rates
380 of PBBs/HBCDDs and PBDEs. Moreover, for the three aforementioned compounds, the concentrations
381 measured in the major part of the sediment cores were not representative of the full extent of the
382 contamination at the time the sediments were deposited. However, the same can be stated for all the

383 other studies regarding BFRs in sediments. Thus, the comparisons based on the existing literature
 384 remain valid.

385 4.2.2. Temporal trends



386

387 Figure 3: Temporal trends of PCBs and legacy BFRs (PBDEs, PBBs, HBCDDs), in $\mu\text{g kg}^{-1}$ dry weight. Points that are represented
 388 in black correspond to the limit of quantification in the sample. European PCBs emissions (Breivik et al., 2002b) and global
 389 PBDEs production (Abbasi et al., 2019) are provided as a comparison. Note that these graphs plotted with a logarithmic scale
 390 can be found in the Supplementary Information (SI-5). [IN COLOUR]

391 The vertical trends of PCBs (Fig. 3.a) showed decreasing concentrations from the 1970s –1980s to 2019
 392 (PDR-1806, PDR-1802, TRS), and stable concentrations in more recent cores (MTE, PDR-1902, PBN-
 393 2002). In all the cores, there was a relatively constant concentration of approximately 10–30 $\mu\text{g kg}^{-1}$
 394 DW from the mid-2000s. These temporal trends are consistent with other observed trends of the
 395 Rhône River (Desmet et al., 2012; Dendievel et al., 2020) and with the data from Breivik et al. (2002b),
 396 which showed that PCB emissions peaked in the 1970s in the European Union and then decreased
 397 steadily.

398 The vertical trends of PBDEs (Fig. 3.b) showed that although the contaminants were detected at very
399 low concentrations in the sediment from the 1970s, the concentrations increased significantly after
400 the mid-1980s. Maximum concentrations were observed in the early 1990s in TRS and MTE. This is not
401 apparent in the graph in Fig.3 because the concentration range in MTE is significantly lower than in the
402 other cores. Additionally, maximum concentrations were observed in the late 1990s in PDR-1902, and
403 in the early 2000s for PDR-1806 and PDR-1802. Decreasing trends were recorded in PBN-2002 from
404 the mid-2000s, which coincided with the decreasing trends observed in the other cores. The temporal
405 trends of cores PDR-1802 and PDR-1806 were found to be the most consistent with PBDE global
406 emissions data from Abbasi et al. (2019); however, all cores showed reasonably good coherence with
407 the temporality of the emissions.

408 HBCDD concentrations were mostly below the LOD before 1990 (Fig. 3.c), and then increased relatively
409 quickly in cores PDR-1806 and PDR-1802. With respect to PDR-1806, the maximum concentration was
410 observed in the mid-2000s, which was consistent with the fact that global HBCDD production peaked
411 in 2006 (Koch et al., 2015). Afterwards, their concentrations decreased quickly and stabilised around
412 1–5 $\mu\text{g kg}^{-1}$ DW from 2010 onwards. While a clear concentration peak was observed only in PDR-1806,
413 HBCDDs in the Rhône River sediments had a clearly defined period of occurrence, that is comprised
414 between 1990 and 2010, based on the results obtained from the four cores.

415 The vertical trend of PBB concentration for cores PDR-1806 and PDR-1802 (Fig. 3.d) showed that
416 maximum PBB concentrations were recorded in the 1970s, followed by a steady decrease. The
417 decreasing trend from 1980 in core TRS also suggested that an earlier peak concentration was not
418 recorded. This is consistent with the fact that PBB production was stopped in 1976 in the USA and from
419 1977 to 2000 in Europe following the accidental contamination of animal feed supplements by PBBs in
420 Michigan (USA). This event highlighted the toxicity of the compounds (Darnerud, 2003). From the mid-
421 2000s, PBB concentrations were low and stable in all three aforementioned cores as well as in PBN-
422 2002. Most PBB concentrations in cores MTE and PDR-1902 were below the LOD (PBN-2002 was

423 characterised by remarkably high limits of quantification), and therefore could not be used for
424 interpretation.

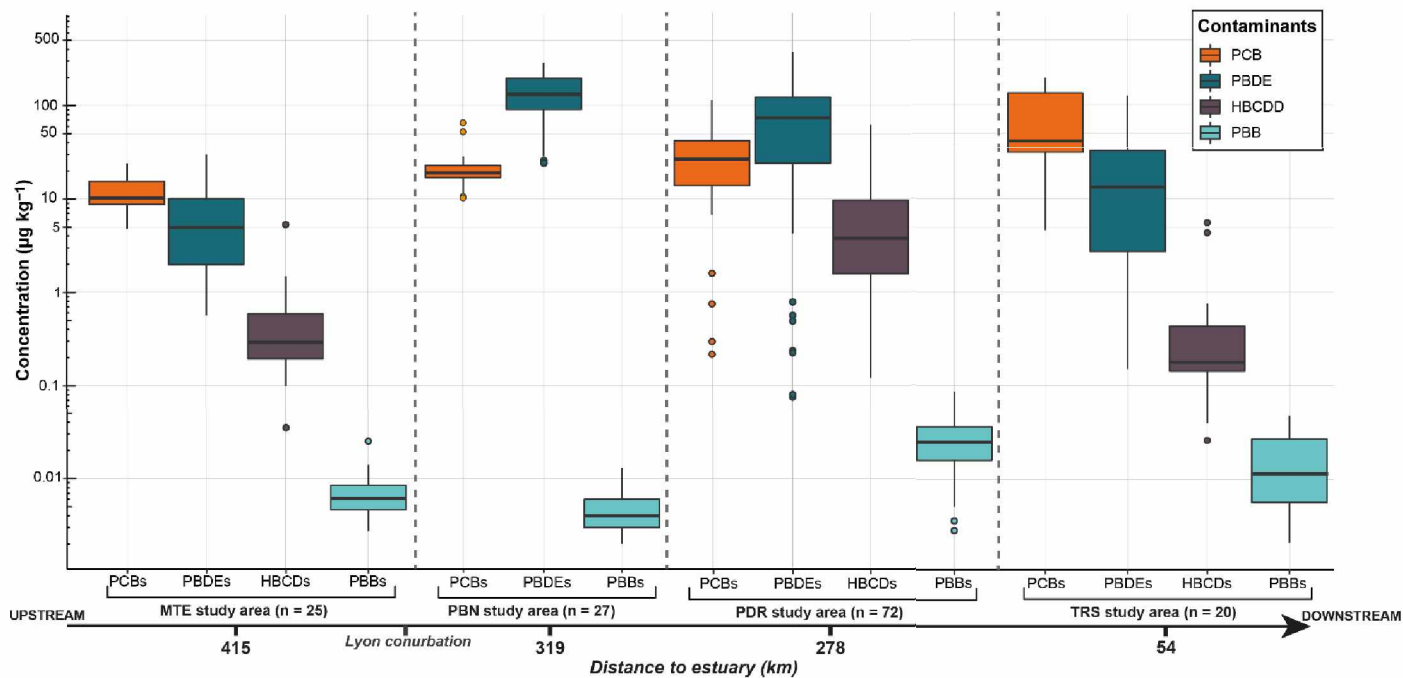
425 Overall, Fig. 3 shows the successive contamination trends of PCBs and legacy BFRs from 1970 to 2000.
426 PCB concentrations decreased in the 1970s as there was a rapid increase and peak of PBB
427 concentrations. In the 1980s, PBDE concentrations increased significantly and peaked in the late 1990s
428 to the early 2000s. Finally, HBCDD concentrations increased in the 1990s and peaked in the mid- to
429 late-2000s. While PBB and HBCDD concentrations rapidly returned to stable background values
430 between 2005 and 2010, the decreasing trend of PBDEs was more gradual. This is likely because they
431 were produced in larger volumes.

432 4.2.3. Spatial trends along the river corridor

433 Boxplots with only quantified concentrations are presented in Fig. 4 for each study area, which allowed
434 to differentiate broad spatial contamination trends along the Rhône River corridor. Three similar
435 boxplots, which were plotted after dividing the concentration data into three groups based on the date
436 of the sample (1969–1990, 1990–2010, and 2010–2019), are available in SI-4. These additional
437 boxplots were constructed to verify whether the varying concentration levels over time would affect
438 the spatial trend along the corridor. However, no significant differences were observed in the spatial
439 trends of the four classes of contaminants between the three time periods (SI-4); therefore, we
440 decided to present only the overall spatial trend over the entire study period (1969–2019; Fig. 4).

441 PCB concentrations steadily increased from the upstream area (MTE, 415 km from the estuary) to the
442 most downstream area (TRS, 54 km from the estuary), although the median concentration range was
443 relatively low (10 to 50 $\mu\text{g kg}^{-1}$ DW). These median concentrations accurately reflected the PCB stock
444 estimated by Dendievel et al. (2020) for the period between 1945 and 2018 along the Rhône River. It
445 should be noted that the time period covered by the different sediment cores also influenced the
446 concentration ranges: for example, PBN-2002 is only for the last 16 years, which means that the peak
447 PCB contamination has not been recorded. This explains the relatively low PCBs concentrations,

448 despite the core being located directly downstream of the Lyon conurbation.



449

450 *Figure 4: Boxplot representation of the concentrations of PCBs and legacy BFRs (PBDEs, PBBs, HBCDDD) in $\mu\text{g.kg}^{-1}$ dry weight*
451 *according to the study area localisation along the Rhône River corridor. [IN COLOUR]*

452 PBDEs followed a different spatial pattern than that of PCBs. While the most upstream area (MTE, 415
453 km from the estuary) still displayed the lowest concentrations, the highest median concentration was
454 found in PBN (319 km from the estuary) at $150 \mu\text{g.kg}^{-1}$ DW; then the concentrations decreased in the
455 next two downstream areas. This could indicate that Lyon and its surrounding urban and industrial
456 areas (329 km from the estuary) are the main sources of PBDE contamination along the corridor, and
457 that PBDEs originating from the metropolis tend to get diluted as they are transported downstream.
458 Indeed, PBDE concentrations in soils and sediments have been shown to correlate positively with
459 urban density (diffuse releases from houses, businesses, and vehicles) and industrial areas, even if the
460 industries are not directly linked to the manufacture or disposal of flame retardants (McGrath et al.,
461 2017). Although most of the Rhône River corridor is anthropized, the Lyon conurbation and the
462 adjacent Chemical Valley represent the most heavily populated and industrialised areas, which could
463 explain the observed spatial trend. In addition, PBDE point sources can be related to manufacturing
464 industries, landfills, incinerators, and recycling facilities (especially e-waste landfills and recycling;

465 McGrath et al., 2017). However, no specific source of this kind was identified near the PBN area,
 466 despite the fact that the Lyon conurbation entails many waste disposal and recycling facilities, which
 467 might have also contributed to the PBDE contamination.

468 The same order of magnitude of HBCDD concentrations was found in the most upstream and
 469 downstream sites, with median concentrations of approximately 0.3 $\mu\text{g kg}^{-1}$ DW in MTE and TRS.
 470 Significantly higher concentrations were found in PDR, 278 km from the estuary (median around 4 μg
 471 kg^{-1} DW), which suggests that HBCDD spatial trends along the Rhône River corridor may be comparable
 472 to PBDEs, although the lack of data in the PBN area makes the comparison difficult.

473 Finally, no clear spatial trend was observed regarding PBB contamination. The concentration variations
 474 in the different areas were possibly related to the time period recorded in the sediment cores; for
 475 example, PBN concentrations could be low because the core dates back to the early 2000s, while most
 476 PBB contamination occurred in the 1970s.

477 4.3. Novel BFRs in the Rhône River sediments

478 4.3.1. Occurrence and contamination levels of nBFRs

479 *Table 2: Occurrence, mean, and median concentrations of nBFRs according to the sediment core, in ng kg⁻¹ dry weight.*

480 *Statistics were computed using all the values. DR = Detection rate; SD = standard deviation. LOD = limit of detection*

Contaminant	PBN-2002 (n = 27)			PDR-1902 (n = 27)			PDR-1806 (n = 21)			PDR-1802 (n = 24)		
	DR	Mean (SD)	Median (min- max)	DR	Mean (SD)	Median (min- max)	DR	Mean (SD)	Median (min- max)	DR	Mean (SD)	Median (min- max)
PBBz	100%	14.59 (5.05)	14.85 (6.65 - 26.29)	100%	12.43 (5.96)	12.38 (4.66 - 33.74)	100%	13.03 (8.62)	12.80 (3.34 - 31.01)	100%	22.41 (9.14)	24.51 (3.35 - 33.88)
PBT	100%	5.6 (7.47)	3.07 (0.8 - 37)	100%	2.16 (2.36)	1.18 (0.20 - 10.84)	100%	25.08 (19.20)	19.33 (4.74 - 87.2.6)	100%	30.40 (16.76)	24.15 (8.18 - 68.46)
TBX	100%	0.7 (0.4)	0.62 (0.27 - 2.18)	100%	0.70 (0.31)	0.62 (0.18 - 1.38)	71%	1.11 (0.95)	1.26 (<LOD - 3.72)	79%	1.49 (2.35)	1.01 (<LOD - 11.86)

HBB	100%	8.97 (3.86)	8.11 (3.14 - 19)	96%	5.55 (3.37)	5.04 (<LOD - 14.06)	100%	27.16 (20.27)	20.45 (7.26 - 68.10)	100%	20.21 (17.31)	15.89 (3.90 - 73.33)
PBEB	52%	0.33 (0.42)	0.044 (<LOD - 1.26)	67%	0.54 (1.15)	0.34 (<LOD - 6.08)	5%	0.15 (0.71)	<LOD (<LOD - 3.2)	13%	1.90 (7.15)	<LOD (<LOD - 34.67)
TBCT	48%	0.3 (0.37)	<LOD (<LOD - 1.15)	7%	0.016 (0.071)	<LOD (<LOD - 0.36)	0%	/	/	0%	/	/
OBT MPI	70%	36.07 (32.63)	30.91 (<LOD - 107.21)	56%	23.34 (28.17)	15.37 (<LOD - 99.15)	0%	/	/	8%	5.72 (19.97)	<LOD (<LOD - 85.23)

481 PBBz, PBT, and HBB were quantified in almost 100% of the samples in the four cores (PBN-2002, PDR-
482 1902, PDR-1806, and PDR-1802) where nBFRs were analysed (Table 2). Out of the aforementioned
483 compounds, PBBz displayed the highest concentrations, with their median concentrations ranging
484 from 12.38 ng kg⁻¹ DW (PBN-1902) to 24.51 ng kg⁻¹ DW (PDR-1802). Maximum concentration was
485 recorded in PDR-1802, that is 33.9 ng kg⁻¹ DW. These levels are similar to PBBz concentrations found
486 in the surface sediments of the Great Lakes of the USA (maximum concentration of 50 ng kg⁻¹ DW; Guo
487 et al., 2020). However, higher PBBz concentrations were found in the soils located inside an e-waste
488 dismantling park in China (median concentrations of 47.9 µg kg⁻¹ DW in the park and 580 ng kg⁻¹ DW
489 nearby; Ge et al., 2020) or around an e-waste recycling workshop in Vietnam (median concentration
490 of 120 ng kg⁻¹ DW and maximum of 560 ng kg⁻¹ DW; Someya et al., 2016).

491 Significant levels of PBT were also found, with median concentrations ranging from 1.18 ng kg⁻¹ DW
492 (PDR-1902) to 24.15 ng kg⁻¹ DW (PDR-1802). Furthermore, the maximum recorded concentration was
493 in PDR-1806, that is 87.26 ng kg⁻¹ DW. These levels are similar to those found in the surface sediments
494 of the Great Lakes, USA (maximum concentration of 90 ng kg⁻¹ DW; Guo et al., 2020), but lower than
495 those found in an e-waste workshop in Vietnam (maximum concentration of 790 ng kg⁻¹ DW, Someya
496 et al., 2016) or in the wetlands close to the industrialised Jiaozhou Bay in China (concentration range
497 of 0.7-1887 µg kg⁻¹ DW; Wang et al., 2015).

498 Median HBB concentrations ranged from 5.04 ng kg⁻¹ DW (PDR-1902) to 20.45 ng kg⁻¹ DW (PDR-1806);
499 the maximum measured concentration was 73.33 ng kg⁻¹ DW in PDR-1802. These levels were similar

500 to those found in surficial sediments in the Thames River of the UK (HBB concentrations $<30 \text{ ng kg}^{-1}$
501 DW; Ganci et al., 2019). However, significantly higher concentrations have been reported in sediments
502 and soils around the world, that is up to $5.56 \text{ } \mu\text{g kg}^{-1}$ DW in the surface sediments of Lake Huron, USA
503 (Guo et al., 2020) and $8.94 \text{ } \mu\text{g kg}^{-1}$ DW in the wetlands of the Jiaozhou Bay, China (Wang et al., 2015).

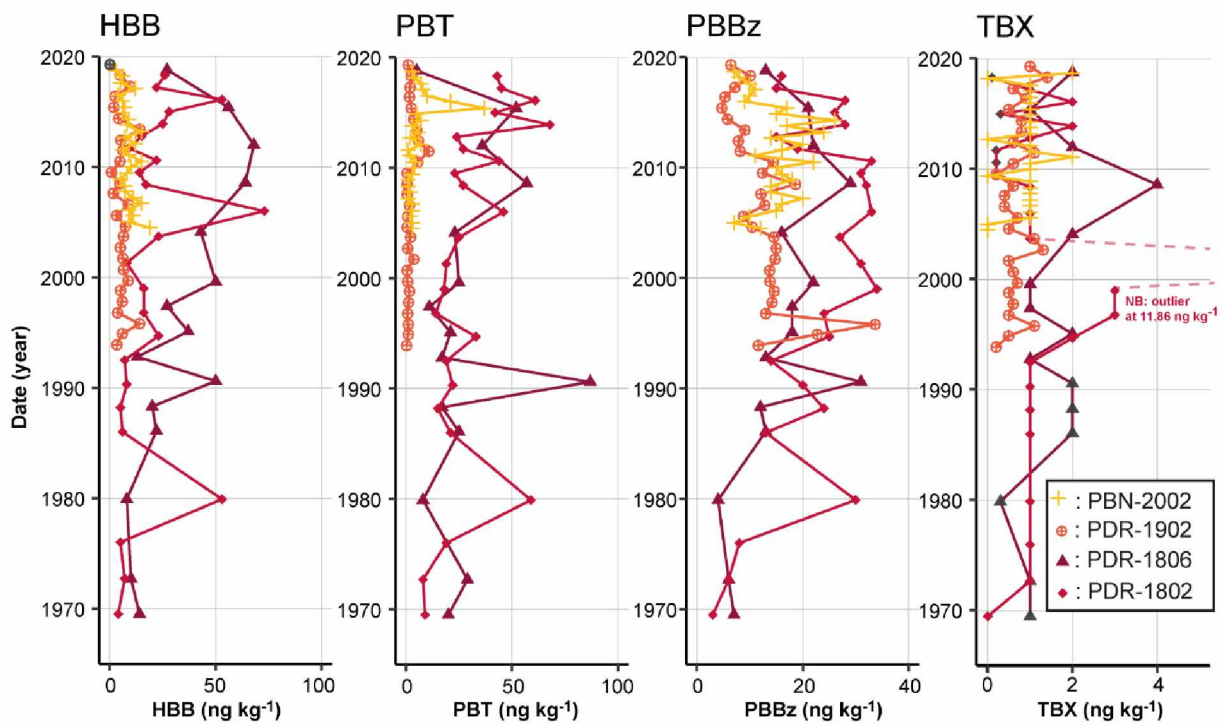
504 TBX was quantified in a majority of the samples, that is 100%, 100%, 71%, and 79% for PBN-2002, PDR-
505 1902, PDR-1806 and PDR-1802, respectively. Moreover, its median concentrations ranged from 0.62
506 to 1.26 ng kg^{-1} DW. Its maximum concentration was 11.86 ng kg^{-1} DW in PDR-1802. These
507 concentrations were in the same order of magnitude as those found in the mangrove surface
508 sediments of Shenzhen, China ($9\text{--}50 \text{ ng kg}^{-1}$ DW; Hu et al., 2020), but significantly lower than those
509 found in the wetlands of the Jiaozhou Bay, China ($0.7\text{--}1.2 \text{ } \mu\text{g kg}^{-1}$ DW; Wang et al., 2015).

510 PBEB, TBCT and OBTMPI were rarely detected, with detection rates ranging from 5% (PDR-1806) to
511 52% (PBN-2002) for PBEB, 0% (PDR-1806 and 1802) to 48% (PBN-2002) for TBCT, and 0% (PDR-1806)
512 to 70% (PBN-2002) for OBTMPI. While the measured concentrations of PBEB and TBCT are significantly
513 low (median concentration $<2 \text{ ng kg}^{-1}$ DW), the OBTMPI levels are similar to the well-quantified nBFRs
514 measured in the four cores, with median concentrations being 15.37 ng kg^{-1} DW and 30.91 ng kg^{-1} DW
515 in PDR-1902 and PBN-2002, respectively. Furthermore, the maximum concentrations in PDR-1902 and
516 PBN-2002 were 107.21 and 99.15 ng kg^{-1} DW, respectively. For comparison, PBEB was measured in the
517 sediments from the Shenzhen Mangrove, China, with concentrations ranging from 6 to 60 ng kg^{-1} DW
518 (Hu et al., 2020) as well as in the sewage sludge in Catalonia, Spain, with concentrations as high as 2.33
519 $\mu\text{g kg}^{-1}$ DW (Gorga et al., 2013). TBCT was rarely detected in the sediments and soils; however, its
520 concentration was $<30 \text{ ng kg}^{-1}$ DW in the San Francisco Bay, USA (Sutton et al., 2019). Similarly, OBTMPI
521 levels in sediments/soils were rarely reported in the literature, but they were found in the soils close
522 to an e-waste recycling workshop in Vietnam at a median concentration of 190 ng kg^{-1} DW (Someya et
523 al., 2016).

524 Overall, the measured concentrations of nBFRs in the Rhône River sediments are of the same order of
525 magnitude as PBBs, but two to four orders of magnitude lower than the concentrations of HBCDDs and
526 PBDEs. While these relatively low concentrations are obviously not indicative of a massive nBFR
527 contamination source along the Rhône River corridor, it is interesting to note that all the investigated
528 compounds were detected and quantified to some extent, including PBEB, TBCT, and OBTMPI which
529 were seldom detected in sediments/soils in previous studies. This might indicate a diffused but non-
530 trivial nBFR contamination in the Rhône River. Additionally, the European Food Safety Authority
531 identified 27 nBFRs in 2013 (EFSA, 2013), and at least 75 different BFRs have been commercialised
532 (Alaee et al., 2003). This indicates that although the nBFRs concentrations are low when considered
533 compound wise, the global contamination load related may be more significant.

534 4.3.2. nBFRs temporal trends

535 Vertical contamination trends were plotted only for the four nBFRs that were detected in more than
536 50% of the samples of the four sediment cores, that is HBB, PBT, PBBz, and TBX (Fig. 5). Although the
537 temporal trends of the aforementioned compounds are vague as compared to the legacy BFRs, the
538 concentrations of HBB, PBT, and PBBz are significant from the late 1970s to the early 1980s. This time
539 period is similar to that of certain legacy BFRs, such as PBDEs. Of the three, PBBz is the only compound
540 with a significantly decreasing trend in the 2010s in all the cores, after reaching its peak in the 1990s–
541 2000s. PBT has showed gradual increase over the years in cores PDR-1806 and PDR-1802. On the other
542 hand, the concentrations cores PBN-2002 and PDR-1902 were low and stable, without significant
543 trends. A clear increase in HBB concentration was observed over time in PDR-1806, with a slight
544 decrease in the 2010s. However, this observation was not corroborated by the three other cores. The
545 concentrations in PDR-1902 and PBN-2002 were low, without significant trends. Additionally, PDR-
546 1802 displayed several concentration peaks from 1980 to 2006, but no clear temporal trend.
547 Meanwhile, TBX appeared in the early 1990s but remained moderate over the entire time period,
548 except for a concentration peak ($12 \text{ ng kg}^{-1} \text{ DW}$) in the early 2000s in PDR-1802.



550

551 *Figure 5: Temporal trends of novel BFRs (HBB, PBT, PBBz, TBX), in ng.kg⁻¹ dry weight. Points that are represented in black*
 552 *correspond to the limit of quantification in the sample. Note that these graphs plotted with a logarithmic scale can be found*
 553 *in the Supplementary Information (SI-7). [IN COLOUR]*

554 Although vertical plots of certain nBFRs were not plotted because they were not systematically
 555 detected in this study, OBTMPI and PBEB were quantified in more than 50% of the samples in the two
 556 most recent cores (PBN-2002 and PDR-1902, cf. Table 2). This indicates that these compounds have
 557 recently appeared in the environment (possibly after 2000). This might be the reason that OBTMPI
 558 and OBEB are among the least studied and the least detected in abiotic environmental matrices (Barón
 559 et al., 2014; Ganci et al., 2019). Overall, although no clear and consistent temporal trends in sediments
 560 for nBFRs were demonstrated in this paper, this first study proved that:

- 561 - Despite the “novel” BFRs appellation, most nBFRs may have been first produced and released
- 562 in the environment between the 1970s and the 1990s i.e., at the same time-period as “legacy
- 563 BFRs”. This is corroborative with the study by Hoh et al. (2005) that shows that PBEB was
- 564 mainly produced in the 1970s and the 1980s in the USA. Besides, while information on the

565 production period of other nBFRs studied in this paper are not readily available, 1,2-Bis(2,4,6-
566 tribromophenoxy)ethane (BTBPE), another nBFR, is known to have been produced since the
567 1970s (Covaci et al., 2011).

568 - However, nBFRs trends in the Rhône River sediments differ from legacy BFRs' because they do
569 not display systematic and significant decreasing concentration trends in the 2010s.

570 Currently, the total number of nBFR molecules produced and released into the environment is
571 unknown, and their screening is relatively uncommon in environmental matrices. However, promising
572 advances in their analysis techniques might help promote their investigation (Bichon et al., 2018).
573 Further research and monitoring efforts are required to ensure that nBFRs do not become a major
574 environmental and sanitary threat as other POPs in the past.

575 5. Conclusion

576 In this study, legacy and novel brominated flame retardants were quantified in dated sediment cores
577 from various locations along the Rhône River corridor in order to reconstruct the temporal trends of
578 the compounds under consideration. A succession of legacy BFRs contamination trends from 1970 to
579 2020 was highlighted: PBBs first appeared in the 1970s but decreased quickly. PBDEs were observed
580 in the mid-1980s, reaching their peak in the late 1990s, and decreasing progressively in the early 2000s.
581 Moreover, HBCDDs increased in the 1990s, peaked in the 2000s, and quickly decreased afterwards. By
582 the late 2010s, following the regulation of their production and use, the aforementioned legacy BFRs
583 reached relatively stable and low concentrations. Overall, legacy BFRs levels in the Rhône River
584 sediments are within the same orders of magnitude as those reported in the literature with respect to
585 other rivers or lakes. Furthermore, they seem to be indicative of diffused but non-trivial BFR
586 contamination that is plausibly linked to the Lyon conurbation and its surrounding industrial areas.
587 Seven nBFRs were also investigated; all of them were detected in the sediments, albeit at
588 concentrations that were two to four orders of magnitude below those of legacy BFRs. While no clear
589 or consistent temporal trends could be identified in our sediment archives, some nBFRs (HBB, PBBz,

590 PBT, and TBX) were estimated to appear in the environment between the 1970s and the 1990s, that
591 is, at the same time period as legacy BFRs. In addition, no significant decrease was observed in their
592 concentrations in recent years, thus emphasising the need for additional investigations regarding
593 nBFRs. Compared to other historical POPs such as PCBs, legacy BFR contamination has been relatively
594 overlooked in the Rhône River as well as worldwide. Furthermore, it is plausible that the contamination
595 of nBFRs has been unnoticed due to their relatively low individual concentrations in the environment.
596 However, the overall contamination load of the nBFRs molecules, which has not been estimated in
597 environmental or ecotoxicological studies, may be more significant, given that not all nBFRs are known
598 or quantifiable. Overall, the lack of knowledge regarding the total number of emerging BFRs, their
599 individual and combined harmful effects, their volume and temporality of production, their sources in
600 the environment, and the absence of regulations regarding their use and production could cause nBFRs
601 to become environmental and health hazards in the near future.

602

603 Acknowledgments:

604 Funding for the work was provided by the European Regional Development Fund (ERDF), Agence de
605 l'eau RMC, CNR, EDF and three regional councils (Auvergne-Rhône-Alpes, PACA and Occitanie) in the
606 context of the Rhône Sediment Observatory (OSR, <http://www.graie.org/osr>). These agencies had no
607 role in the study design nor in the collection, analysis, or interpretation of the data and were not
608 involved in the writing of the article. We confirm that all listed authors were involved in the study and
609 read and approved the final submitted version of the manuscript.

610

611 Reference list:

- 612 Abbasi, G., Li, L., Breivik, K., 2019. Global Historical Stocks and Emissions of PBDEs. *Environ. Sci.*
613 *Technol.* 53, 6330–6340. <https://doi.org/10.1021/acs.est.8b07032>
- 614 Alaei, M., Arias, P., Sjödin, A., Bergman, A., 2003. An overview of commercially used brominated
615 flame retardants, their applications, their use patterns in different countries/regions and

616 possible modes of release. *Environment International* 29, 683–689.
617 [https://doi.org/10.1016/S0160-4120\(03\)00121-1](https://doi.org/10.1016/S0160-4120(03)00121-1)

618 Anim, A.K., Drage, D.S., Goonetilleke, A., Mueller, J.F., Ayoko, G.A., 2017. Distribution of PBDEs,
619 HBCDs and PCBs in the Brisbane River estuary sediment. *Marine Pollution Bulletin* 120, 165–
620 173. <https://doi.org/10.1016/j.marpolbul.2017.05.002>

621 ANSES, 2017. Note relative à l'état des connaissances sur les usages, les sources d'exposition et la
622 toxicité de plusieurs substances de la famille des polybromés [WWW Document]. URL
623 <https://www.anses.fr/fr/system/files/SUBSTANCES2009SA0331Ra-Tome1.pdf> (accessed
624 5.15.20).

625 Aslan, A., 2013. FLUVIAL ENVIRONMENTS | Sediments, in: Elias, S.A., Mock, C.J. (Eds.), *Encyclopedia*
626 *of Quaternary Science* (Second Edition). Elsevier, Amsterdam, pp. 663–675.
627 <https://doi.org/10.1016/B978-0-444-53643-3.00111-4>

628 Bábek, O., Hilscherová, K., Nehyba, S., Zeman, J., Famera, M., Francu, J., Holoubek, I., MacHát, J.,
629 Klánová, J., 2008. Contamination history of suspended river sediments accumulated in oxbow
630 lakes over the last 25 years: Morava River (Danube catchment area), Czech Republic. *Journal of*
631 *Soils and Sediments* 8, 165–176. <https://doi.org/10.1007/s11368-008-0002-8>

632 Barón, E., Santín, G., Eljarrat, E., Barceló, D., 2014. Occurrence of classic and emerging halogenated
633 flame retardants in sediment and sludge from Ebro and Llobregat river basins (Spain). *Journal of*
634 *Hazardous Materials* 265, 288–295. <https://doi.org/10.1016/j.jhazmat.2013.10.069>

635 Barriault, D., Sylvestre, M., 1993. Factors affecting PCB degradation by an implanted bacterial strain
636 in soil microcosms. *Canadian Journal of Microbiology*. <https://doi.org/10.1139/m93-086>

637 Bergman, Å., Rydén, A., Law, R.J., de Boer, J., Covaci, A., Alaee, M., Birnbaum, L., Petreas, M., Rose,
638 M., Sakai, S., Van den Eede, N., van der Veen, I., 2012. A novel abbreviation standard for
639 organobromine, organochlorine and organophosphorus flame retardants and some
640 characteristics of the chemicals. *Environment International* 49, 57–82.
641 <https://doi.org/10.1016/j.envint.2012.08.003>

642 Bethemont, J., Bravard, J.-P., Pour saluer le Rhône. Editions Libel, Lyon (France).

643 Bichon, E., Guiffard, I., Vénisseau, A., Lesquin, E., Vaccher, V., Marchand, P., Le Bizec, B., 2018.
644 Simultaneous analysis of historical, emerging and novel brominated flame retardants in food
645 and feed using a common extraction and purification method. *Chemosphere* 205, 31–40.
646 <https://doi.org/10.1016/j.chemosphere.2018.04.070>

647 Bigus, P., Tobiszewski, M., Namieśnik, J., 2014. Historical records of organic pollutants in sediment
648 cores. *Marine Pollution Bulletin* 78, 26–42. <https://doi.org/10.1016/j.marpolbul.2013.11.008>

649 Blott, S.J., Pye, K., 2001. GRADISTAT: a grain size distribution and statistics package for the analysis of
650 unconsolidated sediments. *Earth Surface Processes and Landforms* 26, 1237–1248.
651 <https://doi.org/10.1002/esp.261>

652 Breivik, K., Sweetman, A., Pacyna, J.M., Jones, K.C., 2002a. Towards a global historical emission
653 inventory for selected PCB congeners — a mass balance approach: 1. Global production and
654 consumption. *Science of The Total Environment* 290, 181–198. [https://doi.org/10.1016/S0048-](https://doi.org/10.1016/S0048-9697(01)01075-0)
655 [9697\(01\)01075-0](https://doi.org/10.1016/S0048-9697(01)01075-0)

- 656 Breivik, K., Sweetman, A., Pacyna, J.M., Jones, K.C., 2002b. Towards a global historical emission
657 inventory for selected PCB congeners — a mass balance approach: 2. Emissions. *Science of The*
658 *Total Environment* 290, 199–224. [https://doi.org/10.1016/S0048-9697\(01\)01076-2](https://doi.org/10.1016/S0048-9697(01)01076-2)
- 659 Chapuis, M., 2012. Bed mobility in highly modified fluvial systems: keys for understanding river
660 management (Durance River, South-Eastern France) (PhD Thesis). Aix-Marseille Université.
- 661 Chi, K.H., Chang, M.B., Kao, S.J., 2007. Historical trends of PCDD/Fs and dioxin-like PCBs in sediments
662 buried in a reservoir in Northern Taiwan. *Chemosphere* 68, 1733–1740.
663 <https://doi.org/10.1016/j.chemosphere.2007.03.043>
- 664 Citterio, A., Piégay, H., 2009. Overbank sedimentation rates in former channel lakes: characterization
665 and control factors. *Sedimentology* 56, 461–482. <https://doi.org/10.1111/j.1365-3091.2008.00979.x>
- 667 Covaci, A., Gerecke, A.C., Law, R.J., Voorspoels, S., Kohler, M., Heeb, N.V., Leslie, H., Allchin, C.R., de
668 Boer, J., 2006. Hexabromocyclododecanes (HBCDs) in the Environment and Humans: A Review.
669 *Environ. Sci. Technol.* 40, 3679–3688. <https://doi.org/10.1021/es0602492>
- 670 Covaci, A., Harrad, S., Abdallah, M.A.-E., Ali, N., Law, R.J., Herzke, D., de Wit, C.A., 2011. Novel
671 brominated flame retardants: A review of their analysis, environmental fate and behaviour.
672 *Environment International* 37, 532–556. <https://doi.org/10.1016/j.envint.2010.11.007>
- 673 Cristale, J., Lacorte, S., Department of Environmental Chemistry, IDAEA-CSIC, Jordi Girona 18-26,
674 08034 Barcelona, Catalonia, Spain, 2015. PBDEs versus NBFR in wastewater treatment plants:
675 occurrence and partitioning in water and sludge. *AIMS Environmental Science* 2, 533–546.
676 <https://doi.org/10.3934/environsci.2015.3.533>
- 677 Cui, S., Fu, Q., Guo, L., Li, Y.-F., Li, T., Ma, W., Wang, M., Li, W., 2016. Spatial–temporal variation,
678 possible source and ecological risk of PCBs in sediments from Songhua River, China: Effects of
679 PCB elimination policy and reverse management framework. *Marine Pollution Bulletin* 106,
680 109–118. <https://doi.org/10.1016/j.marpolbul.2016.03.018>
- 681 Darnerud, P.O., 2003. Toxic effects of brominated flame retardants in man and in wildlife.
682 *Environment International* 29, 841–853. [https://doi.org/10.1016/S0160-4120\(03\)00107-7](https://doi.org/10.1016/S0160-4120(03)00107-7)
- 683 Davis, J.W., Gonsior, S., Marty, G., Ariano, J., 2005. The transformation of hexabromocyclododecane
684 in aerobic and anaerobic soils and aquatic sediments. *Water Research* 39, 1075–1084.
685 <https://doi.org/10.1016/j.watres.2004.11.024>
- 686 de Wit, C.A., 2002. An overview of brominated flame retardants in the environment. *Chemosphere*
687 46, 583–624. [https://doi.org/10.1016/S0045-6535\(01\)00225-9](https://doi.org/10.1016/S0045-6535(01)00225-9)
- 688 de Wit, C.A., Herzke, D., Vorkamp, K., 2010. Brominated flame retardants in the Arctic environment
689 — trends and new candidates. *Science of The Total Environment* 408, 2885–2918.
690 <https://doi.org/10.1016/j.scitotenv.2009.08.037>
- 691 Dendievel, A.-M., Mourier, B., Coynel, A., Evrard, O., Labadie, P., Ayrault, S., Debret, M., Koltalo, F.,
692 Copard, Y., Faivre, Q., Gardes, T., Vauclin, S., Budzinski, H., Grosbois, C., Winiarski, T., Desmet,
693 M., 2020. Spatio-temporal assessment of the polychlorinated biphenyl (PCB) sediment
694 contamination in four major French river corridors (1945–2018). *Earth System Science Data* 12,
695 1153–1170. <https://doi.org/10.5194/essd-12-1153-2020>

- 696 Desmet, M., Mourier, B., Mahler, B.J., Van Metre, P.C., Roux, G., Persat, H., Lefèvre, I., Peretti, A.,
697 Chapron, E., Simonneau, A., Miège, C., Babut, M., 2012. Spatial and temporal trends in PCBs in
698 sediment along the lower Rhône River, France. *Science of The Total Environment* 433, 189–197.
699 <https://doi.org/10.1016/j.scitotenv.2012.06.044>
- 700 Directive 2002/95/CE du Parlement européen et du Conseil du 27 janvier 2003 relative à la limitation
701 de l'utilisation de certaines substances dangereuses dans les équipements électriques et
702 électroniques, 2003, 2002/95/CE.
- 703 Drage, D., Mueller, J.F., Birch, G., Eaglesham, G., Hearn, L.K., Harrad, S., 2015. Historical trends of
704 PBDEs and HBCDs in sediment cores from Sydney estuary, Australia. *Science of The Total
705 Environment* 512–513, 177–184. <https://doi.org/10.1016/j.scitotenv.2015.01.034>
- 706 EFSA (European Food Safety and Authority), 2013. Scientific Opinion on Emerging and Novel
707 Brominated Flame Retardants (BFRs) in Food. Parma, Italy.
- 708 Evenset, A., Christensen, G.N., Carroll, J., Zaborska, A., Berger, U., Herzke, D., Gregor, D., 2007.
709 Historical trends in persistent organic pollutants and metals recorded in sediment from Lake
710 Ellasjøen, Bjørnøya, Norwegian Arctic. *Environmental Pollution* 146, 196–205.
711 <https://doi.org/10.1016/j.envpol.2006.04.038>
- 712 FAO (Food and Agriculture Organization of the United Nations), 2000. Assessing soil contamination. A
713 reference manual (No. 8), FAO PESTICIDE DISPOSAL SERIES.
- 714 Ganci, A.P., Vane, C.H., Abdallah, M.A.-E., Moehring, T., Harrad, S., 2019. Legacy PBDEs and NBFRs in
715 sediments of the tidal River Thames using liquid chromatography coupled to a high resolution
716 accurate mass Orbitrap mass spectrometer. *Science of The Total Environment* 658, 1355–1366.
717 <https://doi.org/10.1016/j.scitotenv.2018.12.268>
- 718 Ge, X., Ma, S., Zhang, X., Yang, Y., Li, G., Yu, Y., 2020. Halogenated and organophosphorous flame
719 retardants in surface soils from an e-waste dismantling park and its surrounding area:
720 Distributions, sources, and human health risks. *Environment International* 139, 105741.
721 <https://doi.org/10.1016/j.envint.2020.105741>
- 722 Gerecke, A.C., Giger, W., Hartmann, P.C., Heeb, N.V., Kohler, H.-P.E., Schmid, P., Zennegg, M., Kohler,
723 M., 2006. Anaerobic degradation of brominated flame retardants in sewage sludge.
724 *Chemosphere* 64, 311–317. <https://doi.org/10.1016/j.chemosphere.2005.12.016>
- 725 Gerecke, A.C., Hartmann, P.C., Heeb, N.V., Kohler, H.-P.E., Giger, W., Schmid, P., Zennegg, M., Kohler,
726 M., 2005. Anaerobic Degradation of Decabromodiphenyl Ether. *Environ. Sci. Technol.* 39, 1078–
727 1083. <https://doi.org/10.1021/es048634j>
- 728 Gorga, M., Martínez, E., Ginebreda, A., Eljarrat, E., Barceló, D., 2013. Determination of PBDEs, HBB,
729 PBEB, DBDPE, HBCD, TBBPA and related compounds in sewage sludge from Catalonia (Spain).
730 *Sci. Total Environ.* 444, 51–59. <https://doi.org/10.1016/j.scitotenv.2012.11.066>
- 731 Guerra, P., Alae, M., Jiménez, B., Pacepavicius, G., Marvin, C., MacInnis, G., Eljarrat, E., Barceló, D.,
732 Champoux, L., Fernie, K., 2012. Emerging and historical brominated flame retardants in
733 peregrine falcon (*Falco peregrinus*) eggs from Canada and Spain. *Environment International* 40,
734 179–186. <https://doi.org/10.1016/j.envint.2011.07.014>
- 735 Guo, J., Li, Z., Ranasinghe, P., Rockne, K.J., Sturchio, N.C., Giesy, J.P., Li, A., 2020. Halogenated flame
736 retardants in sediments from the Upper Laurentian Great Lakes: Implications to long-range

737 transport and evidence of long-term transformation. *Journal of Hazardous Materials* 384,
738 121346. <https://doi.org/10.1016/j.jhazmat.2019.121346>

739 Hagemann, L., Buchty-Lemke, M., Maaß, A.-L., Schüttrumpf, H., Lehmkuhl, F., Schwarzbauer, J., 2019.
740 Potential hotspots of persistent organic pollutants in alluvial sediments of the meandering
741 Wurm River, Germany. *Journal of Soils and Sediments*. [https://doi.org/10.1007/s11368-019-](https://doi.org/10.1007/s11368-019-02491-4)
742 [02491-4](https://doi.org/10.1007/s11368-019-02491-4)

743 Hassan, Y., Shoeib, T., 2015. Levels of polybrominated diphenyl ethers and novel flame retardants in
744 microenvironment dust from Egypt: An assessment of human exposure. *Science of The Total*
745 *Environment* 505, 47–55. <https://doi.org/10.1016/j.scitotenv.2014.09.080>

746 Hoh, E., Zhu, L., Hites, R.A., 2005. Novel flame retardants, 1,2-bis(2,4,6-tribromophenoxy)ethane and
747 2,3,4,5,6-pentabromoethylbenzene, in United States' environmental samples. *Environ. Sci.*
748 *Technol.* 39, 2472–2477. <https://doi.org/10.1021/es048508f>

749 Hu, Y., Sun, Y., Pei, N., Zhang, Z., Li, H., Wang, W., Xie, J., Xu, X., Luo, X., Mai, B., 2020.
750 Polybrominated diphenyl ethers and alternative halogenated flame retardants in mangrove
751 plants from Futian National Nature Reserve of Shenzhen City, South China. *Environmental*
752 *Pollution* 260, 114087. <https://doi.org/10.1016/j.envpol.2020.114087>

753 IARC, 2016. Polychlorinated Biphenyls and Polybrominated Biphenyls, IARC Monographs on the
754 Evaluation of Carcinogenic Risks to Humans, vol. 107. Lyon (France).

755 Jinhui, L., Yuan, C., Wenjing, X., 2017. Polybrominated diphenyl ethers in articles: a review of its
756 applications and legislation. *Environ Sci Pollut Res* 24, 4312–4321.
757 <https://doi.org/10.1007/s11356-015-4515-6>

758 Karickhoff, S.W., Brown, D.S., Scott, T.A., 1979. Sorption of hydrophobic pollutants on natural
759 sediments. *Water Research* 13, 241–248. [https://doi.org/10.1016/0043-1354\(79\)90201-X](https://doi.org/10.1016/0043-1354(79)90201-X)

760 Kim, Y.R., Harden, F.A., Toms, L.-M.L., Norman, R.E., 2014. Health consequences of exposure to
761 brominated flame retardants: A systematic review. *Chemosphere* 106, 1–19.
762 <https://doi.org/10.1016/j.chemosphere.2013.12.064>

763 Koch, C., Schmidt-Kötters, T., Rupp, R., Sures, B., 2015. Review of hexabromocyclododecane (HBCD)
764 with a focus on legislation and recent publications concerning toxicokinetics and -dynamics.
765 *Environmental Pollution* 199, 26–34. <https://doi.org/10.1016/j.envpol.2015.01.011>

766 Kohler, M., Zennegg, M., Bogdal, C., Gerecke, A.C., Schmid, P., V. Heeb, N., Sturm, M., Vonmont, H.,
767 E. Kohler, H.-P., Giger, W., 2008. Temporal Trends, Congener Patterns, and Sources of Octa-,
768 Nona-, and Decabromodiphenyl Ethers (PBDE) and Hexabromocyclododecanes (HBCD) in Swiss
769 Lake Sediments. *Environ. Sci. Technol.* 42, 6378–6384. <https://doi.org/10.1021/es702586r>

770 La Guardia, M.J., Hale, R.C., Newman, B., 2013. Brominated Flame-Retardants in Sub-Saharan Africa:
771 Burdens in Inland and Coastal Sediments in the eThekweni Metropolitan Municipality, South
772 Africa. *Environ. Sci. Technol.* 47, 9643–9650. <https://doi.org/10.1021/es4020212>

773 Law, R.J., Alaei, M., Allchin, C.R., Boon, J.P., Lebeuf, M., Lepom, P., Stern, G.A., 2003. Levels and
774 trends of polybrominated diphenylethers and other brominated flame retardants in wildlife.
775 *Environment International* 29, 757–770. [https://doi.org/10.1016/S0160-4120\(03\)00110-7](https://doi.org/10.1016/S0160-4120(03)00110-7)

- 776 Law, R.J., Allchin, C.R., de Boer, J., Covaci, A., Herzke, D., Lepom, P., Morris, S., Tronczynski, J., de Wit,
777 C.A., 2006. Levels and trends of brominated flame retardants in the European environment.
778 *Chemosphere* 64, 187–208. <https://doi.org/10.1016/j.chemosphere.2005.12.007>
- 779 Law, R.J., Covaci, A., Harrad, S., Herzke, D., Abdallah, M.A.-E., Fernie, K., Toms, L.-M.L., Takigami, H.,
780 2014. Levels and trends of PBDEs and HBCDs in the global environment: Status at the end of
781 2012. *Environment International* 65, 147–158. <https://doi.org/10.1016/j.envint.2014.01.006>
- 782 Li, P., Wu, H., Li, Q., Jin, J., Wang, Y., 2015. Brominated flame retardants in food and environmental
783 samples from a production area in China: concentrations and human exposure assessment.
784 *Environ Monit Assess* 187, 719. <https://doi.org/10.1007/s10661-015-4947-y>
- 785 Liber, Y., Mourier, B., Marchand, P., Bichon, E., Perrodin, Y., Bedell, J.-P., 2019. Past and recent state
786 of sediment contamination by persistent organic pollutants (POPs) in the Rhône River:
787 Overview of ecotoxicological implications. *Science of The Total Environment* 646, 1037–1046.
788 <https://doi.org/10.1016/j.scitotenv.2018.07.340>
- 789 Lorgeoux, C., Moilleron, R., Gasperi, J., Ayrault, S., Bonté, P., Lefèvre, I., Tassin, B., 2016. Temporal
790 trends of persistent organic pollutants in dated sediment cores: Chemical fingerprinting of the
791 anthropogenic impacts in the Seine River basin, Paris. *Science of The Total Environment* 541,
792 1355–1363. <https://doi.org/10.1016/j.scitotenv.2015.09.147>
- 793 Marvin, C.H., Tomy, G.T., Armitage, J.M., Arnot, J.A., McCarty, L., Covaci, A., Palace, V., 2011.
794 Hexabromocyclododecane: Current Understanding of Chemistry, Environmental Fate and
795 Toxicology and Implications for Global Management. *Environ. Sci. Technol.* 45, 8613–8623.
796 <https://doi.org/10.1021/es201548c>
- 797 McGrath, T.J., Ball, A.S., Clarke, B.O., 2017. Critical review of soil contamination by polybrominated
798 diphenyl ethers (PBDEs) and novel brominated flame retardants (NBFRs); concentrations,
799 sources and congener profiles. *Environmental Pollution* 230, 741–757.
800 <https://doi.org/10.1016/j.envpol.2017.07.009>
- 801 McGrath, T.J., Morrison, P.D., Ball, A.S., Clarke, B.O., 2018. Concentrations of legacy and novel
802 brominated flame retardants in indoor dust in Melbourne, Australia: An assessment of human
803 exposure. *Environment International* 113, 191–201.
804 <https://doi.org/10.1016/j.envint.2018.01.026>
- 805 Minh, N.H., Isobe, T., Ueno, D., Matsumoto, K., Mine, M., Kajiwara, N., Takahashi, S., Tanabe, S.,
806 2007. Spatial distribution and vertical profile of polybrominated diphenyl ethers and
807 hexabromocyclododecanes in sediment core from Tokyo Bay, Japan. *Environmental Pollution*
808 148, 409–417. <https://doi.org/10.1016/j.envpol.2006.12.011>
- 809 Möller, A., Xie, Z., Sturm, R., Ebinghaus, R., 2011. Polybrominated diphenyl ethers (PBDEs) and
810 alternative brominated flame retardants in air and seawater of the European Arctic.
811 *Environmental Pollution* 159, 1577–1583. <https://doi.org/10.1016/j.envpol.2011.02.054>
- 812 Mourier, B., Desmet, M., Van Metre, P.C., Mahler, B.J., Perrodin, Y., Roux, G., Bedell, J.-P., Lefèvre, I.,
813 Babut, M., 2014. Historical records, sources, and spatial trends of PCBs along the Rhône River
814 (France). *Science of The Total Environment* 476, 568–576.
815 <https://doi.org/10.1016/j.scitotenv.2014.01.026>
- 816 Muir, D.C.G., Rose, N.L., 2007. Persistent Organic Pollutants in the Sediments of Lochnagar, in: Rose,
817 N.L. (Ed.), *Lochnagar: The Natural History of a Mountain Lake*, Developments in

- 818 Paleoenvironmental Research. Springer Netherlands, Dordrecht, pp. 375–402.
819 <https://doi.org/10.1007/1-4020-3986-7> 16
- 820 Nylund, K., Asplund, L., Jansson, B., Jonsson, P., Litzén, K., Sellström, U., 1992. Analysis of some
821 polyhalogenated organic pollutants in sediment and sewage sludge. *Chemosphere* 24, 1721–
822 1730. [https://doi.org/10.1016/0045-6535\(92\)90227-l](https://doi.org/10.1016/0045-6535(92)90227-l)
- 823 Oh, J.K., Kotani, K., Managaki, S., Masunaga, S., 2014. Levels and distribution of
824 hexabromocyclododecane and its lower brominated derivative in Japanese riverine
825 environment. *Chemosphere* 109, 157–163.
826 <https://doi.org/10.1016/j.chemosphere.2014.01.074>
- 827 Olivier, J.-M., Dole-Olivier, M.-J., Amoros, C., Carrel, G., Malard, F., Lamouroux, N., Bravard, J.-P.,
828 2009. Chapter 7 - The Rhône River Basin, in: Tockner, K., Uehlinger, U., Robinson, C.T. (Eds.),
829 Rivers of Europe. Academic Press, London, pp. 247–295. <https://doi.org/10.1016/B978-0-12-369449-2.00007-2>
- 830
- 831 Piégay, H., Hupp, C.R., Citterio, A., Dufour, S., Moulin, B., Walling, D.E., 2008. Spatial and temporal
832 variability in sedimentation rates associated with cutoff channel infill deposits: Ain River,
833 France. *Water Resources Research* 44. <https://doi.org/10.1029/2006WR005260>
- 834 Poma, G., Roscioli, C., Guzzella, L., 2014. PBDE, HBCD, and novel brominated flame retardant
835 contamination in sediments from Lake Maggiore (Northern Italy). *Environ Monit Assess* 186,
836 7683–7692. <https://doi.org/10.1007/s10661-014-3959-3>
- 837 Pont, D., Simonnet, J.-P., Walter, A.V., 2002. Medium-term Changes in Suspended Sediment Delivery
838 to the Ocean: Consequences of Catchment Heterogeneity and River Management (Rhône River,
839 France). *Estuarine, Coastal and Shelf Science* 54, 1–18. <https://doi.org/10.1006/ecss.2001.0829>
- 840 Poulhier, G., Launay, M., Le Bescond, C., Thollet, F., Coquery, M., Le Coz, J., 2019. Combining flux
841 monitoring and data reconstruction to establish annual budgets of suspended particulate
842 matter, mercury and PCB in the Rhône River from Lake Geneva to the Mediterranean Sea.
843 *Science of The Total Environment* 658, 457–473.
844 <https://doi.org/10.1016/j.scitotenv.2018.12.075>
- 845 Prevedouros, K., Jones, K.C., Sweetman, A.J., 2004. Estimation of the Production, Consumption, and
846 Atmospheric Emissions of Pentabrominated Diphenyl Ether in Europe between 1970 and 2000.
847 *Environ. Sci. Technol.* 38, 3224–3231. <https://doi.org/10.1021/es049711d>
- 848 Sedláček, J., Bábek, O., Kielar, O., 2016. Sediment accumulation rates and high-resolution
849 stratigraphy of recent fluvial suspension deposits in various fluvial settings, Morava River
850 catchment area, Czech Republic. *Geomorphology* 254, 73–87.
851 <https://doi.org/10.1016/j.geomorph.2015.11.011>
- 852 Shi, T., Chen, S.-J., Luo, X.-J., Zhang, X.-L., Tang, C.-M., Luo, Y., Ma, Y.-J., Wu, J.-P., Peng, X.-Z., Mai, B.-
853 X., 2009. Occurrence of brominated flame retardants other than polybrominated diphenyl
854 ethers in environmental and biota samples from southern China. *Chemosphere* 74, 910–916.
855 <https://doi.org/10.1016/j.chemosphere.2008.10.047>
- 856 Someya, M., Suzuki, G., Ionas, A.C., Tue, N.M., Xu, F., Matsukami, H., Covaci, A., Tuyen, L.H., Viet,
857 P.H., Takahashi, S., Tanabe, S., Takigami, H., 2016. Occurrence of emerging flame retardants
858 from e-waste recycling activities in the northern part of Vietnam. *Emerging Contaminants*,

- 859 Special Issue: A Tribute to Hidetaka Takigami 2, 58–65.
860 <https://doi.org/10.1016/j.emcon.2015.10.002>
- 861 Stockholm Convention, 2018. Stockholm convention on Persistent Organic Pollutants. Text and
862 annexes, revised in 2017 (SSC). Châtelaine (Switzerland).
- 863 Sundström, G., Hutzinger, O., Safe, S., 1976. Identification of 2,2',4,4',5,5'-hexabromobiphenyl as the
864 major component of flame retardant fireMaster®BP-6. *Chemosphere* 5, 11–14.
865 [https://doi.org/10.1016/0045-6535\(76\)90049-7](https://doi.org/10.1016/0045-6535(76)90049-7)
- 866 Sutton, R., Chen, D., Sun, J., Greig, D.J., Wu, Y., 2019. Characterization of brominated, chlorinated,
867 and phosphate flame retardants in San Francisco Bay, an urban estuary. *Science of The Total*
868 *Environment* 652, 212–223. <https://doi.org/10.1016/j.scitotenv.2018.10.096>
- 869 Tanabe, S., 2008. Temporal trends of brominated flame retardants in coastal waters of Japan and
870 South China: Retrospective monitoring study using archived samples from es-Bank, Ehime
871 University, Japan. *Marine Pollution Bulletin* 57, 267–274.
872 <https://doi.org/10.1016/j.marpolbul.2007.12.017>
- 873 Van Ael, E., Covaci, A., Blust, R., Bervoets, L., 2012. Persistent organic pollutants in the Scheldt
874 estuary: Environmental distribution and bioaccumulation. *Environment International* 48, 17–27.
875 <https://doi.org/10.1016/j.envint.2012.06.017>
- 876 Van Metre, P.C., Babut, M., Mourier, B., Mahler, B.J., Roux, G., Desmet, M., 2015. Declining Dioxin
877 Concentrations in the Rhone River Basin, France, Attest to the Effectiveness of Emissions
878 Controls. *Environ. Sci. Technol.* 49, 12723–12730. <https://doi.org/10.1021/acs.est.5b03416>
- 879 Vane, C.H., Ma, Y.-J., Chen, S.-J., Mai, B.-X., 2010. Increasing polybrominated diphenyl ether (PBDE)
880 contamination in sediment cores from the inner Clyde Estuary, UK. *Environ Geochem Health* 32,
881 13–21. <https://doi.org/10.1007/s10653-009-9261-6>
- 882 Vauclin, S., Mourier, B., Dendievel, A.-M., Noclin, N., Piégay, H., Marchand, P., Vénisseau, A., de
883 Vismes, A., Lefèvre, I., Winiarski, T., 2020. Depositional environments and historical
884 contamination as a framework to reconstruct fluvial sedimentary evolution. *Science of The*
885 *Total Environment* 142900. <https://doi.org/10.1016/j.scitotenv.2020.142900>
- 886 Vénisseau, A., Bichon, E., Brosseaud, A., Vaccher, V., Lesquin, E., Larvor, F., Durand, S., Dervilly-Pinel,
887 G., Marchand, P., Le Bizec, B., 2018. Occurrence of legacy and novel brominated flame
888 retardants in food and feed in France for the period 2014 to 2016. *Chemosphere* 207, 497–506.
889 <https://doi.org/10.1016/j.chemosphere.2018.05.122>
- 890 Vetter, W., Gallistl, C., Schlien, A., Preston, T., Müller, J., von der Trenck, K.T., 2017. Brominated
891 flame retardants (BFRs) in eggs from birds of prey from Southern Germany, 2014.
892 *Environmental Pollution* 231, 569–577. <https://doi.org/10.1016/j.envpol.2017.08.047>
- 893 Wang, L., Zhao, Q., Zhao, Y., Zheng, M., Lou, Y., Yang, B., 2015. New non-PBDE brominated flame
894 retardants in sediment and plant samples from Jiaozhou Bay wetland. *Marine Pollution Bulletin*
895 97, 512–517. <https://doi.org/10.1016/j.marpolbul.2015.05.026>
- 896 Wu, J.-P., Guan, Y.-T., Zhang, Y., Luo, X.-J., Zhi, H., Chen, S.-J., Mai, B.-X., 2011. Several current-use,
897 non-PBDE brominated flame retardants are highly bioaccumulative: Evidence from field
898 determined bioaccumulation factors. *Environment International* 37, 210–215.
899 <https://doi.org/10.1016/j.envint.2010.09.006>

900 Xiong, P., Yan, X., Zhu, Q., Qu, G., Shi, J., Liao, C., Jiang, G., 2019. A Review of Environmental
901 Occurrence, Fate, and Toxicity of Novel Brominated Flame Retardants. *Environ. Sci. Technol.* 53,
902 13551–13569. <https://doi.org/10.1021/acs.est.9b03159>

903 Yang, R., Wei, H., Guo, J., Li, A., 2012. Emerging Brominated Flame Retardants in the Sediment of the
904 Great Lakes. *Environ. Sci. Technol.* 46, 3119–3126. <https://doi.org/10.1021/es204141p>

905 Yu, Y., Hung, H., Alexandrou, N., Roach, P., Nordin, K., 2015. Multiyear Measurements of Flame
906 Retardants and Organochlorine Pesticides in Air in Canada’s Western Sub-Arctic. *Environ. Sci.*
907 *Technol.* 49, 8623–8630. <https://doi.org/10.1021/acs.est.5b01996>

908 Zhang, X.-L., Luo, X.-J., Liu, H.-Y., Yu, L.-H., Chen, S.-J., Mai, B.-X., 2011. Bioaccumulation of Several
909 Brominated Flame Retardants and Dechlorane Plus in Waterbirds from an E-Waste Recycling
910 Region in South China: Associated with Trophic Level and Diet Sources. *Environ. Sci. Technol.*
911 45, 400–405. <https://doi.org/10.1021/es102251s>

912 Zhang, Y., Ruan, Y., Sun, H., Zhao, L., Gan, Z., 2013. Hexabromocyclododecanes in surface sediments
913 and a sediment core from Rivers and Harbor in the northern Chinese city of Tianjin.
914 *Chemosphere* 90, 1610–1616. <https://doi.org/10.1016/j.chemosphere.2012.08.037>

915 Zhu, L.Y., Hites, R.A., 2005. Brominated Flame Retardants in Sediment Cores from Lakes Michigan and
916 Erie. *Environ. Sci. Technol.* 39, 3488–3494. <https://doi.org/10.1021/es048240s>

917

918

919 Supplementary Information

920 *SI-1: Coordinates and characteristics of the six studied sediment cores.*

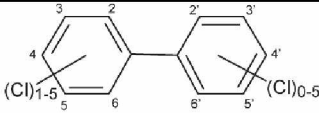
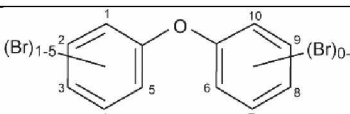
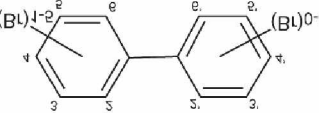
Core	Study site typology	Total length (cm)	X coordinate (WGS 84)	Y coordinate (WGS 84)	Covered time-period
MTE	Secondary channel	101	5.554050	45.701585	1984-2018
PBN-2002	Owbow lake	108	4.824724	4.654604	2004-2020
PDR-1802	Secondary channel	94	4.76651	45.33100	1969-2018
PDR-1806	Secondary channel	82	4.760209	45.344806	1968-2018
PDR-1902	Dam reservoir	104	4.7552535	45.3821711	1993-2019
TRS	Secondary channel	300	4.618433	43.725261	1981-2017

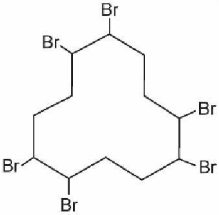
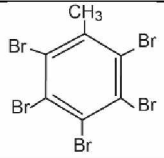
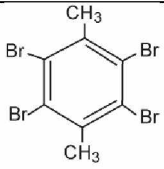
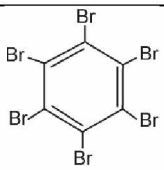
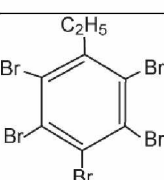
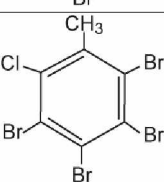
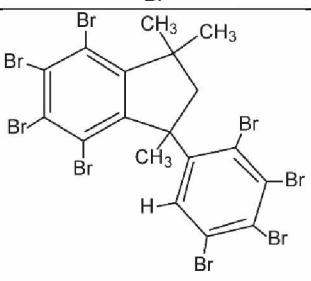
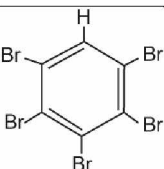
921

922

923 *SI-2: CAS number, abbreviations according to Bergman et al. (2012) and structure of the studied molecules. NB: molecules indicated with an asterisk (*) were not listed in Bergman et al. (2012).*

924

CAS number	Practical abbreviation according to Bergman et al., 2012 (used in the manuscript)	Structural abbreviation according to Bergman et al., 2012	Chemical abstract name	Structure	13C-labeled internal standards used	Limits of detection ($\mu\text{g kg}^{-1}$)
1336-36-3	PCBs *	/	Polychlorinated biphenyls		13C-PCB28, 13C-PCB52, 13C-PCB101, 13C-PCB118, 13C-PCB138, 13C-PCB-153, 13CPCB-180	0.049 (PCB118) – 0.109 (PCB28)
/	PBDEs	/	Polybrominated diphenyl ethers		13C-BDE28, 13C-BDE47, 13C-BDE99, 13C-BDE100, 13C-BDE153, 13C-BDE154, 13C-BDE183, 13C-BDE209	0.00002 (BDE28) – 0.05 (BDE183)
/	PBBs	/	Polybrominated biphenyls		13C-PBB153	0.00005 (PBB52) – 0.0062 (PBB101)

3194-55-6	HBCDD	HxBcDD	Cyclododecane, 1,2,5,6,9,10- hexabromo-		13C- α HBCDD, 13C- β HBCDD, 13C- γ HBCDD	0.002- 0.136
87-83-2	PBT	PeBT	Benzene, 1,2,3,4,5- pentabromo-6- methyl		13C-PBBz	0.00001 - 0.00023
23488-38- 2	TBX	TeBDiMeBz	Benzene, 1,2,4,5- tetrabromo-3,6- dimethyl		13C-PBBz	0.00002 - 0.00019
87-82-1	HBB	HxBBz	Benzene, 1,2,3,4,5,6- hexabromo-		13C-HBB	0.00006 - 0.00258
85-22-3	PBEb	PeBEtBz	Benzene, 1,2,3,4,5- pentabromo-6- ethyl-		13C-PBBz	0.00004 - 0.00031
39569-21- 6	TBCT	TeBCMeBz	Benzene, 1,2,3,4- tetrabromo-5- chloro-6-mehtyl		13C-PBBz	0.00001 - 0.00041
1084889- 51-9- 1025956- 65- 3893843- 07-7	OBTMPI	OBTrMePhIn	1 H-Indene, 4,5,6,7- tetrabromo-2,3- dihydro- 1,1,3- trimethyl-3- (2,3,4,5- tetrabromophe nyl)-		13C-BDE209	0.00798 - 0.04782
608-90-2	PBBz *	/	Benzene, 1,2,3,4,5- pentabromo		13C-PBBz	0.00002 - 0.00041

925

926

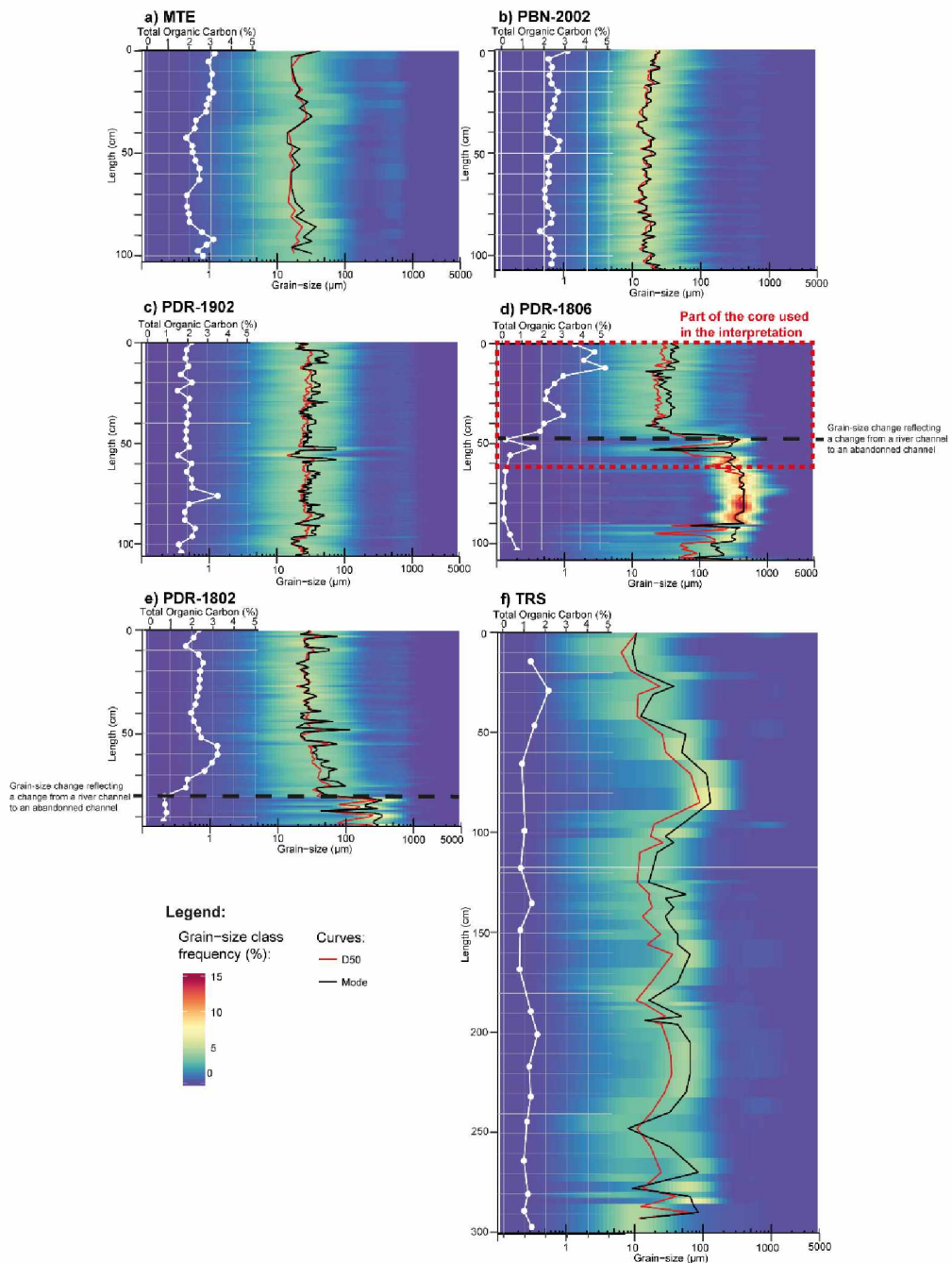
927

928

929 *SI-3: Model type and parameters used to compute the age-depth model of core PBN-2002.*

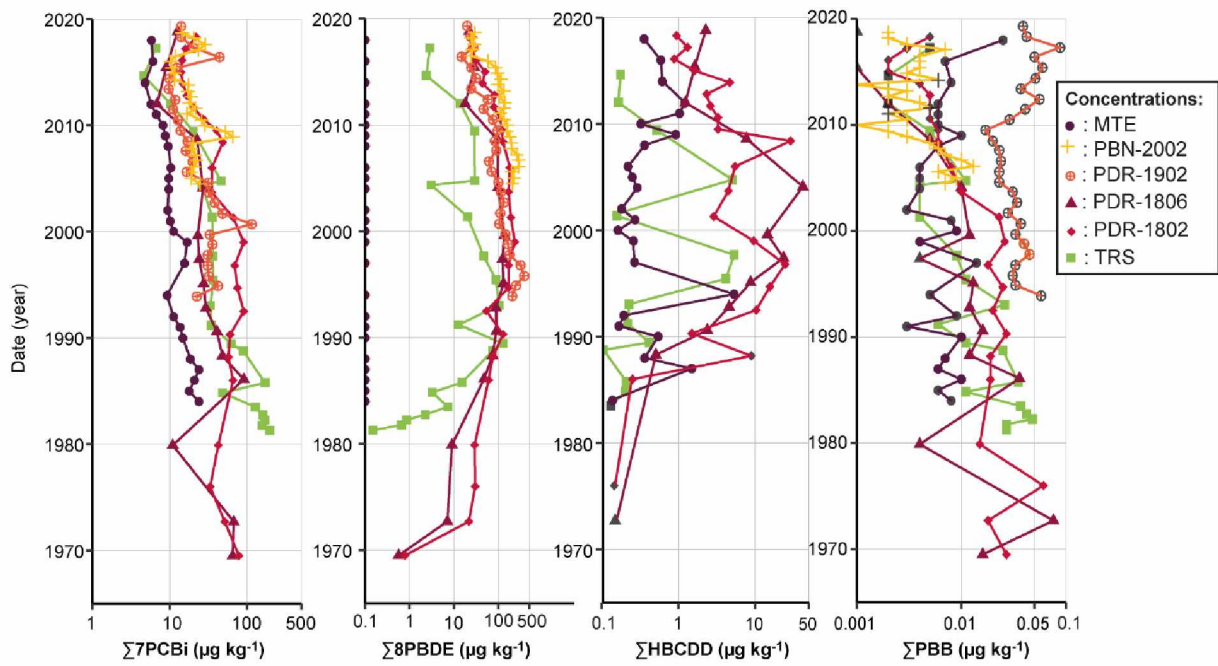
PBN-2002 – Type of model: linear regression			
Time-marker	Date (years)	Depth (cm)	Standard error (years)
Core sampling	2020	0	1
PBDE interdiction	2008	80	4
Date of the bottom of the core based on ²¹⁰ Pbxs regression	2004	104	4

930



931

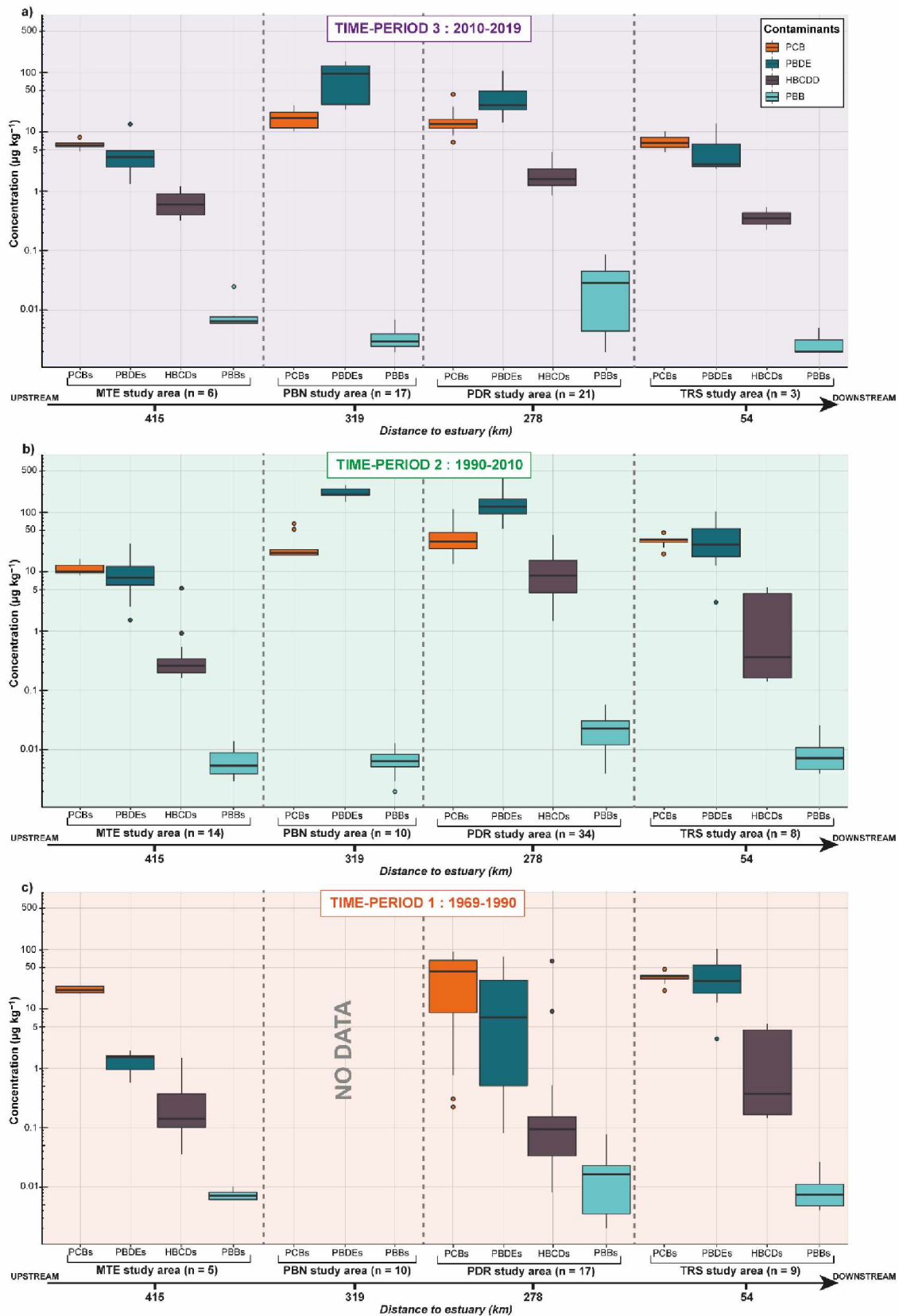
932 *SI-4: Grain-size distribution and total organic carbon content of the six studied sediment cores.*



933

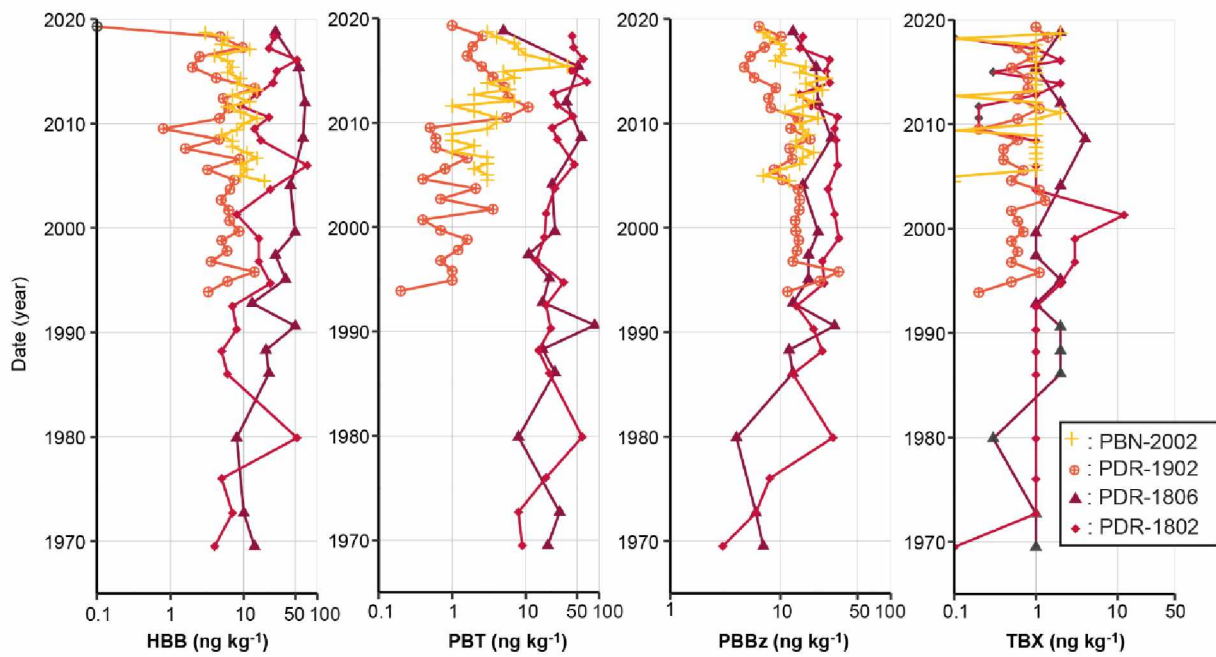
934 *SI-5: Temporal trends of PCBs and legacy BFRs (PBDEs, PBBs, HBCDDs) represented with a logarithmic scale in $\mu\text{g kg}^{-1}$ dry*

935 *weight. Points that are represented in black correspond to the limit of quantification in the sample.*



936

937 *SI-6: Boxplot representation of the concentrations in PCBs and legacy BFRs (PBDEs, PBBs, HBCDDD) in µg kg⁻¹ dry weight*
 938 *according to the study area localization along the Rhône River corridor. a) for the 2010-2019 time-period; b) for the 1990-*
 939 *2010 time-period; c) for the 1969-1990 time-period.*

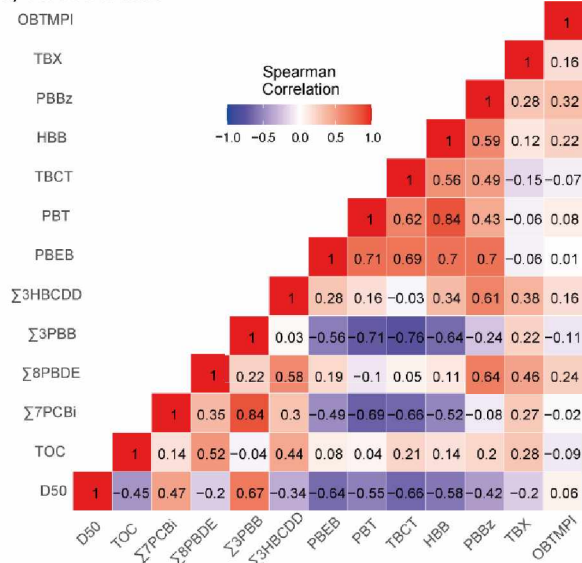


940

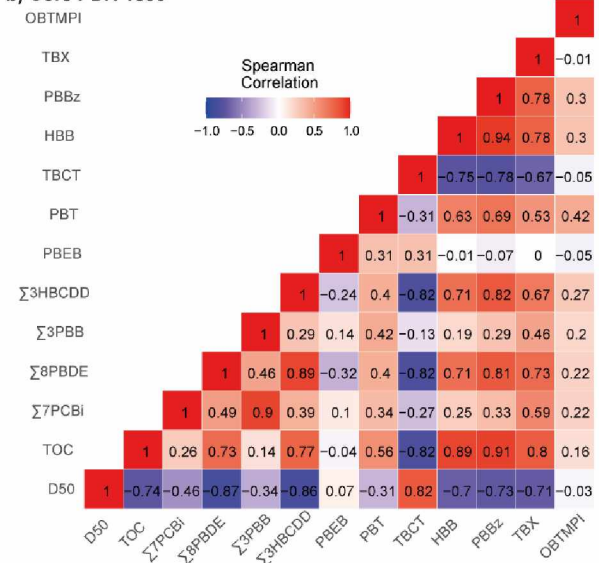
941 *SI-7: Temporal trends of novel BFRs (HBB, PBT, PBBz, and TBX) represented with a logarithmic scale in ng kg^{-1} dry weight.*

942 *Points that are represented in black correspond to the limit of quantification in the sample.*

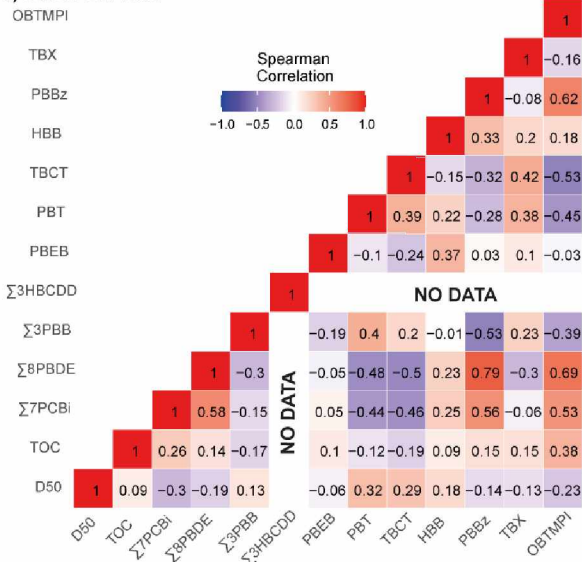
a) Core PDR-1802



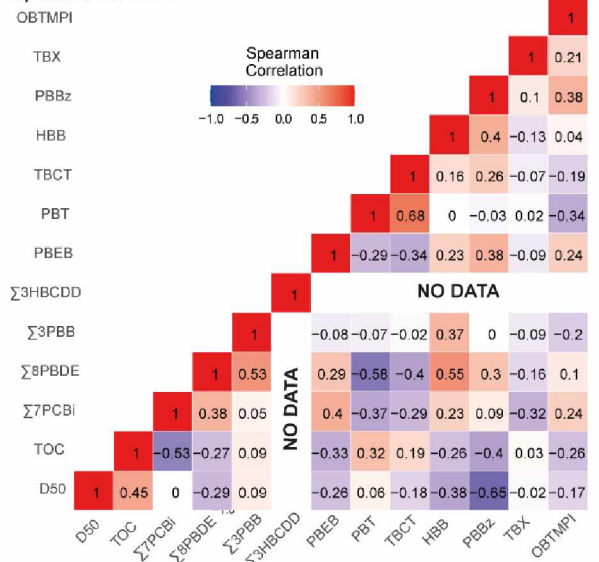
b) Core PDR-1806



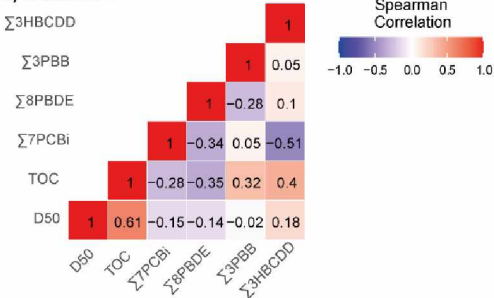
c) Core PDR-1902



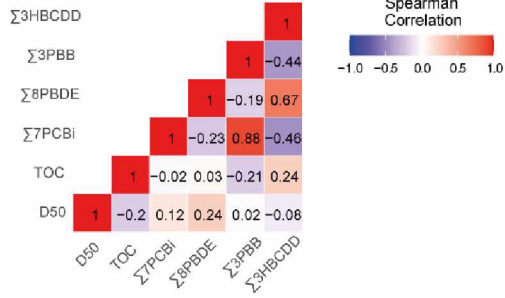
d) Core PBN-2002



e) Core MTE



f) Core TRS



943

944

945

SI-8: Spearman correlations matrices between the analysed contaminants, Total Organic Carbon (TOC) and grain size (D50) for a) core PDR-1802, b) core PDR-1806, c) core PDR-1902, d) core PBN-2002, e) core MTE, f) core TRS.